A. E. KAVUR

IZMIR KATIP CELEBI UNIVERSITY

2018

IZMIR KATIP CELEBI UNIVERSITY
GRADUATE SCHOOL OF NATURAL AND APPLIED SCIENCES

DESIGN AND IMPLEMENTATION OF CHAOTIC DELTA ROBOT MIXER SYSTEM FOR PREPARING GRAPHENE NANOCOMPOSITE COATING

M.Sc. THESIS

Ali Emre KAVUR

Department of Biomedical Technologies

SEPTEMBER 2018

IZMIR KATIP CELEBI UNIVERSITY
GRADUATE SCHOOL OF NATURAL AND APPLIED SCIENCES

DESIGN AND IMPLEMENTATION OF CHAOTIC DELTA ROBOT MIXER SYSTEM FOR PREPARING GRAPHENE NANOCOMPOSITE COATING

M.Sc. THESIS

Ali Emre KAVUR
(Y140101011)

Department of Biomedical Technologies

Thesis Advisor: Assoc. Prof. Savaş ŞAHİN

SEPTEMBER 2018

İZMİR KATİP ÇELEBİ ÜNİVERSİTESİ
FEN BİLİMLERİ ENSTİTÜSÜ

GRAFEN NANOKOMPOZİT KAPLAMA HAZIRLANMASI İÇİN KAOTİK SİSTEM TABANLI GÜRBÜZ DELTA ROBOT SIVI KARIŞTIRICI TASARIMI VE GERÇEKLEMESİ

YÜKSEK LİSANS TEZİ

Ali Emre KAVUR
(Y140101011)

Biyomedikal Teknolojileri Ana Bilim Dalı

Tez Danışmanı: Doç. Dr. Savaş ŞAHİN

EYLÜL 2018

Ali Emre KAVUR, a **M.Sc.** student of **IKCU Graduate School of Natural And Applied Sciences**, successfully defended the thesis entitled "**DESIGN AND IMPLEMENTATION OF CHAOTIC DELTA ROBOT MIXER SYSTEM FOR PREPARING GRAPHENE NANOCOMPOSITE COATING**", which he prepared after fulfilling the requirements specified in the associated legislations, before the jury whose signatures are below.

Thesis Advisor :

Assoc. Prof. Savaş ŞAHİN .....
İzmir Katip Çelebi University

Jury Members :

Assoc. Prof. M. Özgür SEYDİBEYOĞLU .....
İzmir Katip Çelebi University

Assist. Prof. M. Emre ÇEK .....
Dokuz Eylül University

Date of Submission : 03.09.2018
Date of Defense : 21.09.2018

To my family,

FOREWORD

First, I would like to express my sincere gratitude to my thesis advisor Assoc. Prof. Savaş ŞAHİN for his support of my study and research. His guidance helped me in all the time of research and writing of this thesis.

I would also like to thank Assoc. Prof. M. Özgür Seydibeyoğlu and his student Sibel Demiroğlu Mustafov who were involved in the experiments for this research project.

My sincere thanks to Cem Baytöre, Levent Taşdöğen and Rıza Gökbunar for their contributions and supports to my study.

I would like to express my sincere thanks to İzmir Katip Çelebi University and TÜBİTAK for supporting my thesis. This thesis was supported by the Scientific and Technological Research Council of Turkey (TÜBİTAK) under Grant 114E432.

September 2018 Ali Emre KAVUR

TABLE OF CONTENTS

Page

ABBREVIATIONS

GUI	**:** Graphical User Interface
FTIR	**:** Fourier Transform Infrared Spectroscopy
XRD	**:** X-ray Diffraction
WCA	**:** Water Contact Angle

LIST OF TABLES

Page

LIST OF FIGURES

Page

DESIGN AND IMPLEMENTATION OF CHAOTIC SYSTEM BASED ROBUST DELTA ROBOT BLENDER

ABSTRACT

This thesis includes design, implementation and polymer nanocomposite mixing application of chaotic system based robust delta robot. Blending fluids is a vital process while preparing coating materials. The most commonly used the coating materials are polymeric materials which need to be blended in non-Newtonian fluids. This process is very critical and harder to achieve a perfectly prepared coating material. To achieve superior blending performance, two different and independent chaotic systems were used to chaotify delta robot-based blender system. One of them was used for chaotification of the propeller while the other chaotic system controls the three-dimensional position of the propeller. The designed and implemented system uses efficiency of the chaotic mixing in terms of homogeneity and operation time related to the consumed electrical energy. The performance of the system was compared to traditional constantly worked blenders and chaotically turned blenders. In these performance evaluations, well known and reliable material characterization methods were used. The obtained results show that, the proposed system has a better mixing performance than other blending systems.

Keywords: Delta robot, chaos, chaotification, robustness, polymer nanocomposites, graphene, mixing

GRAFEN NANOKOMPOZİT KAPLAMA HAZIRLANMASI İÇİN KAOTİK SİSTEM TABANLI GÜRBÜZ DELTA ROBOT SIVI KARIŞTIRICI TASARIMI VE GERÇEKLEMESİ

ÖZET

Bu tez kaotik sistem tabanlı delta robot karıştırıcının tasarlanmasını ve polimer nanokompozitlerin etkin karıştırılmasına uygulanmasını içermektedir. Kaplama malzemesi üretiminde maddelerin etkin karıştırılması kritik öneme sahip bir süreçtir. Kapmama malzemelerinin büyük çoğunluğu non-Newtonian tipteki sıvılarla karıştırılması gereken polimetrik materyallerden oluşmaktadır. Mükemmel şekilde karıştırılmış bir kaplama malzemesi elde edilebilmesi için bu işlem oldukça zorlayıcı ve kritik öneme sahiptir. Daha üstün bir karıştırma performansı elde etmek amacıyla bu tezde sunulan karıştırıcı sistemin kaotik olarak çalışması için iki farklı ve birbirlerinden bağımsız kaotik sistem kullanılmıştır. Bu sistemlerden bir tanesi karıştırıcı şaftın ucundaki pervanenin hızını kontrol ederken, diğer sistem ise bu pervanenin üç boyutlu eksendeki koordinatlarını kontrol etmektedir. Proje kapsamında üretilen bu sistem, bilimsel yazında mevcut olan sabit konumlu ancak hızı kaotik olarak değişen sistemleri bir ileri seviyeye taşımakta ve kaotik sistemlerin zaman verimliliğini daha etkin olarak kullanmaktadır. Sistemin performansı değerlendirilirken sabit hızla çalışan geleneksel karıştırma yöntemleri ve sabit konumlu ancak kaotik hızda çalışan karıştırma sistemleri ile karşılaştırılmıştır. Bu performans değerlendirilmesi için güvenilir ve sıkça kullanılan malzeme karakterizasyon yöntemleri kullanılmıştır. Elde edilen bulgular önerilen ve gerçekleştirilen kaotik sistem tabanlı delta robot karıştırıcının performansının diğer sistemlerden daha başarılı olduğunu ortaya koymuştur.

Anahtar Kelimeler: Delta robot, kaos, kaotikleştirme; gürbüzlük, polimer nanokompozit, grafen

1. INTRODUCTION

The process of mixing fluids in industrial applications is defined as a critical engineering problem. This problem is a popular research topic in scientific area [1]. In contrast to conventional mixing techniques, it is possible to obtain more homogeneous mixtures in shorter time with chaotic mixers [2]. In this thesis, a new blender system based on two independent chaotic systems was designed and implemented to build a chaotic system-based delta robot. It provides a new approach to meet industrial blending needs and being robust against disruptive effects. It has a stable and time efficient structure.

The delta robot concept was created as a solution to a faster palletizing of a chocolate factory in 1985 [3]. The workers in the factory were responsible of palletization of chocolates. However, this process needs certain concentration. Also, it may be a stressful process. In order to handle this problem, it was thought that a robot mechanism might be used. However, there was no industrial robot mechanism that can be adapted to the factory to solve this problem at that time. A new designed solution, such as Delta robot [4], was needed. The delta robot design depends on using parallelograms which creates ability of an output link to stay at an absolute position with respect to an input link [5]. The design that includes three parallelograms stays the orientation of the mobile platform constant [6].

Different industrial applications are using the delta robot. Among these food industry [7], the delta robot is also used in other fields; for instance, to robot-assisted surgery systems [8; 9], 3D printers [10; 11], artificial organs [12] and nanotechnology fields [13; 14].

In 20th century, nanotechnology and nanocomposites are one of the most innovative technologies in many distinctive engineering disciplines such as electronic industry, biomedical materials and material science [15; 16] as well as medical applications [17; 18; 19]. In nanotechnological applications, successful dispersion of nanoparticles in

the polymer matrices is a very critical process for preparation of nanocomposites. However, this is one of the most difficult process in the commercialization of nanocomposites such as producing coating materials.

Fluids can be classified in two different methods. One of them is their behavior under pressure. In this method fluids are called ‘compressible’ and ‘incompressible’ fluids [20]. A second classification is to cluster fluids depends on their response to an applied shear stress rate. Here, fluids are classified "Newtonian" and "non-Newtonian" fluids [20]. The shear stress and the shear rate of a Newtonian fluid has a linear relation. In contrast with Newtonian fluids, a non-Newtonian fluid has a different relation between the shear stress and the shear rate. In other words, if a fluid shows different behavior than Newton's law of viscosity, it can be called non-Newtonian fluid [21]. Non-Newtonian fluids' viscosity is related with shear rate [22]. Example of non-Newtonian fluids are; toothpaste, blood, ketchup, coating materials, molten polymers.

Coating is a process which is commonly used to apply uniform thin solid layers to flat surfaces [23]. One of the most common application of coating is spin coating in industrial fields [24; 25; 26]. Coating has also critical role for dental [27], and biomedical [28] applications. In many cases, the coating material is polymeric material. It needs to be diluted in a solution. Coating materials may be obtained by blending a nanocomposite material and non-Newtonian fluids. Therefore, coating flow of non-Newtonian fluids is a widely researched area in many years [29]. An effective method for blending non-Newtonian fluids and polymers has very critical importance for industrial applications.

In addition with all difficulties in industrial blending systems, blending non-Newtonian fluids is also harder process and needs more sophisticated systems [30]. For this reason, constantly positioned blenders are insufficient to mix such liquids effectively. Chaotic system based mixers have better performance than constantly positioned blenders for this type of liquid mixture [2; 31; 32; 33]. The proposed system in this thesis has shown a better mixing performance than the conventional blending systems in the related literature because the proposed system was driven by two different and independent chaotic systems. Both the speed of the blender shaft and the position of the propeller are instantly driven by chaotic systems. In addition to this

proposed technique, robust control methods have also been applied to the system to protect the system from external or interfering effects.

The proposed chaotic system-based delta robot mixer, shown in Figure 1.1, was used for mixing graphene nanoplatelets with polymer materials. The results obtained from these mixtures were used to measure the performance of the system. The samples obtained from the mixtures were analyzed by using material characterization techniques which are frequently used in the literature and reliable [34; 35].

This thesis includes all the steps of the thesis which are presented as; Literature review, Materials and methods, and Conclusion.

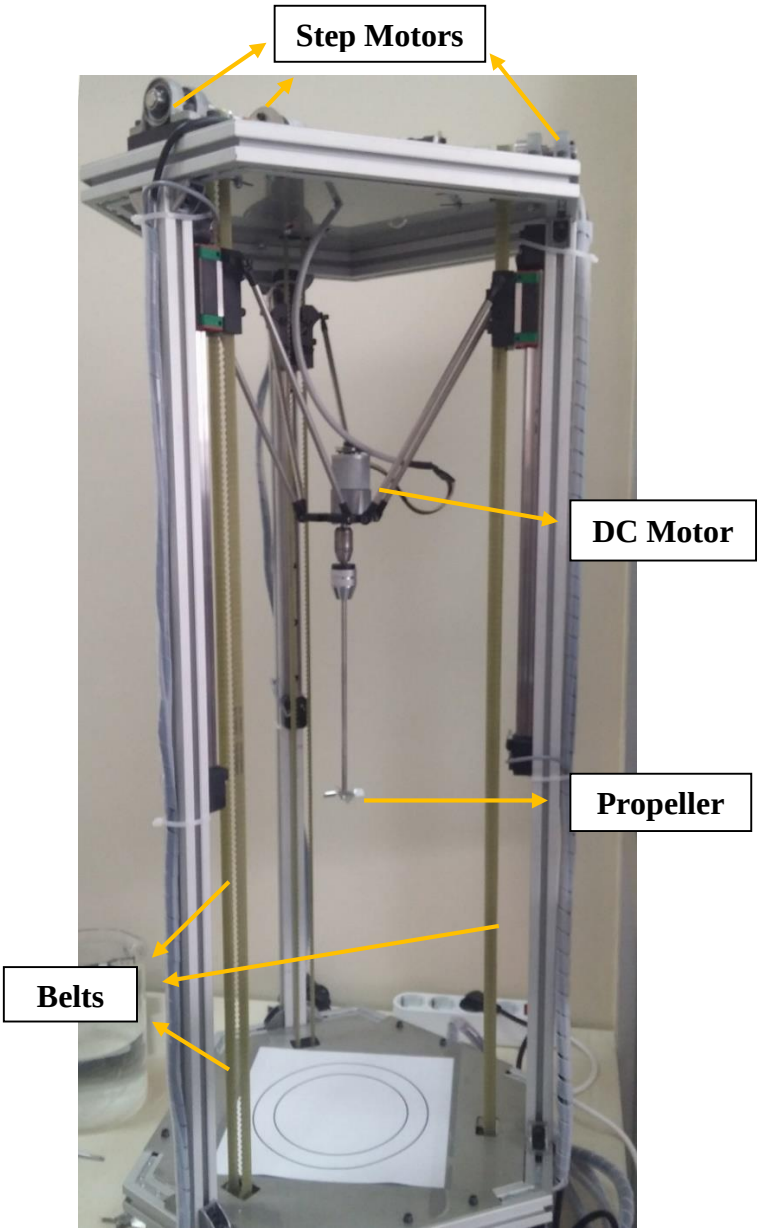

Figure 1.1 : Side view of Delta Robot Liquid Blender.

2. LITERATURE REVIEW

The delta robot blender has two independent sub-systems. One of them is its blending speed while other one is the position of the propeller in beaker. That is why; two chaotic systems are needed to drive both the speed of the propeller shaft and the chaotically changing of its coordinates in 3D space. For this reason, the chaotic systems in the literature have been examined with related reference documents. In this chapter a brief explanation of chaotic systems is presented. After that the outputs of five well-known chaotic systems have been analyzed for the selection of the chaotic systems to be used in the system. These are; Lorenz, Chua, Newton-Leipnik, Chen and Rössler chaotic systems. The main motivation for choosing these system is that they are most well-known used chaotic systems which have three independent state variables.

2.1 Definition of Chaos and Lorenz Chaotic System

In the following fifty years, many developments have been made about the chaotic systems. In literature, there is not universally accepted definition of *chaos* yet. Steven Strogatz defines chaos in his book with these definition: *"**Chaos** is aperiodic long-term behavior in a deterministic system that exhibits sensitive dependence on initial conditions* [36]*."* This definition explains that there are not any random inputs in chaotic systems. The system is very dependent to initial conditions. When the system reaches to infinity, the trajectories do not locate to specific points. In other words, trajectories do not have a periodic orbit.

The first usage of the chaotic systems was made by Edward Norton Lorenz in 1963 [37]. Lorenz was a meteorologist and tried to explain some of the unreliable weather actions. He decided to design a system of differential equations to solve this problem. Lorenz looked at a two-dimensional liquid cell that was warmed from beneath and cooled from above. The liquid movement can be expressed by an arrangement of

differential conditions including too many factors. Lorenz accepted that everything constant except three of factors stayed independent variables. These are, the rate of convective "overturning" (x), the horizontal and vertical temperature variation (y and z, respectively). The resulted motion is defined by three-dimensional system of differential equations. The three parameters are; the Prandtl number a, the Rayleigh number r , and b which determines the size of the system. After these simplifications were made, the differential equations system defined as:

$$\begin{aligned} \dot{x} &= -ax + ay \\ \dot{y} &= rx - y - xz \\ \dot{z} &= -bz + xy \end{aligned} \qquad [1]$$

x, y, and z define state variables. Lorenz chaotic system is sensitive to its parameters. In this thesis, the constants and variables were selected and simulated according to original article [37]. These are; a=10, b=8/3 and r=28. Result of the equation set with these coefficients, the output of each equation is plotted in Figure 2.1 in three dimensions on the x-y-z axis.

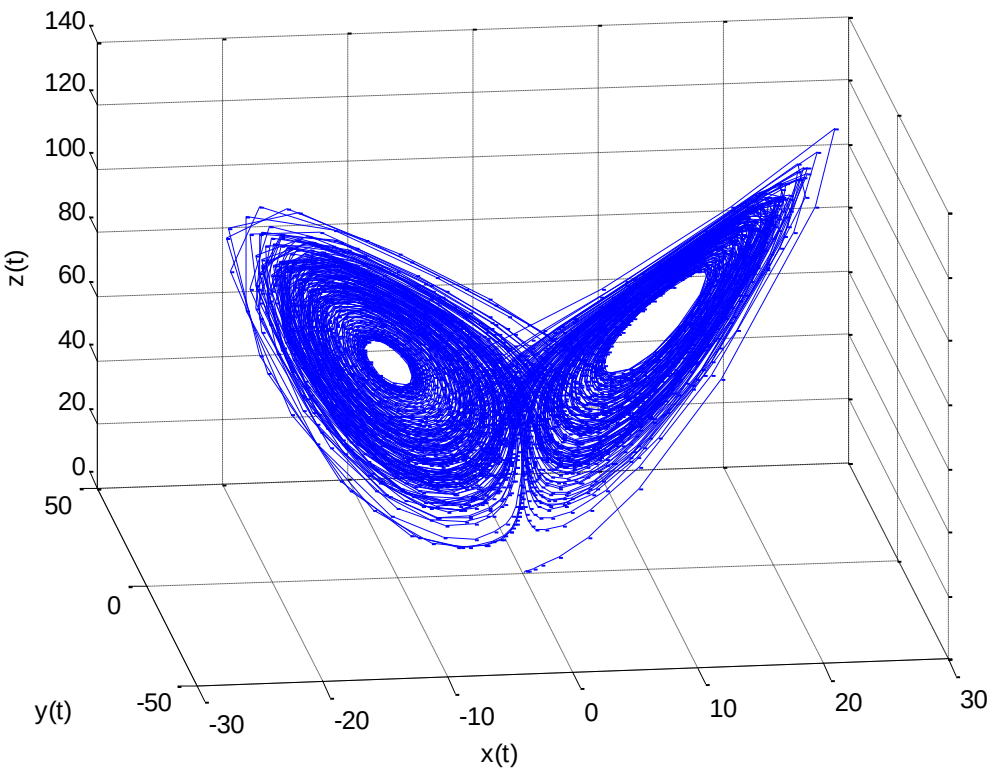

Figure 2.1 : Simulation output of Lorenz chaotic system in 3D axis.

2.2 Chua's Circuit

Chua's circuit was developed by Leon O. Chua in 1983. The circuit shows chaotic behaviors. The circuit shown in Figure 2.2, includes one non-linear resistance (N_R on the right), capacitor, inductor etc.

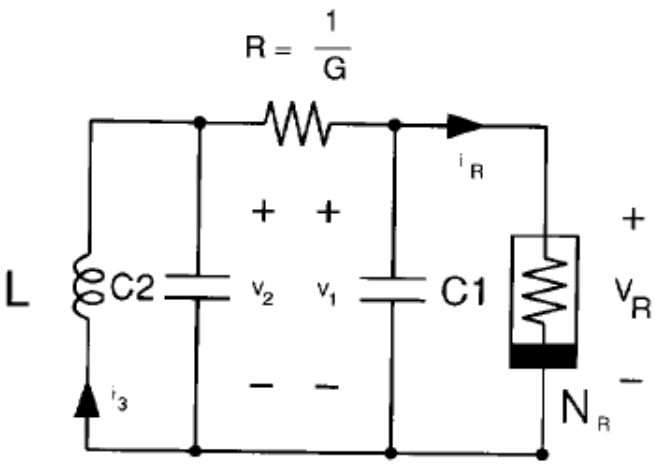

Figure 2.2 : Chua's Circuit (Taken from original article [38]).

If Kirchhoff's current and voltage equations are applied in the Chua Circuit, three sets of nonlinear differential equations are obtained. The form the Chua chaotic system given in Eq. 2:

$$\dot{x} = \alpha(y - x - f(x))$$
$$\dot{y} = x - y + z$$
$$\dot{z} = -\beta y \qquad [2]$$
$$\mathrm{f(x)} = \mathrm{m_0 x} + \frac{1}{2}(\mathrm{m_1} - \mathrm{m_0})[|\mathrm{x}+1| - |\mathrm{x}-1|]$$

The state variables are defined by x, y, and z while α, $\beta, \mathrm{m_0}, \mathrm{m_1}$ are constants. $f(x)$ symbolizes response of non-linear resistance in the circuit. According to trials and calculations, $\alpha = 10.725$ and $\beta = 10.593$ selected. The result of the equation set with the use of these coefficients is plotted in Figure 2.3:

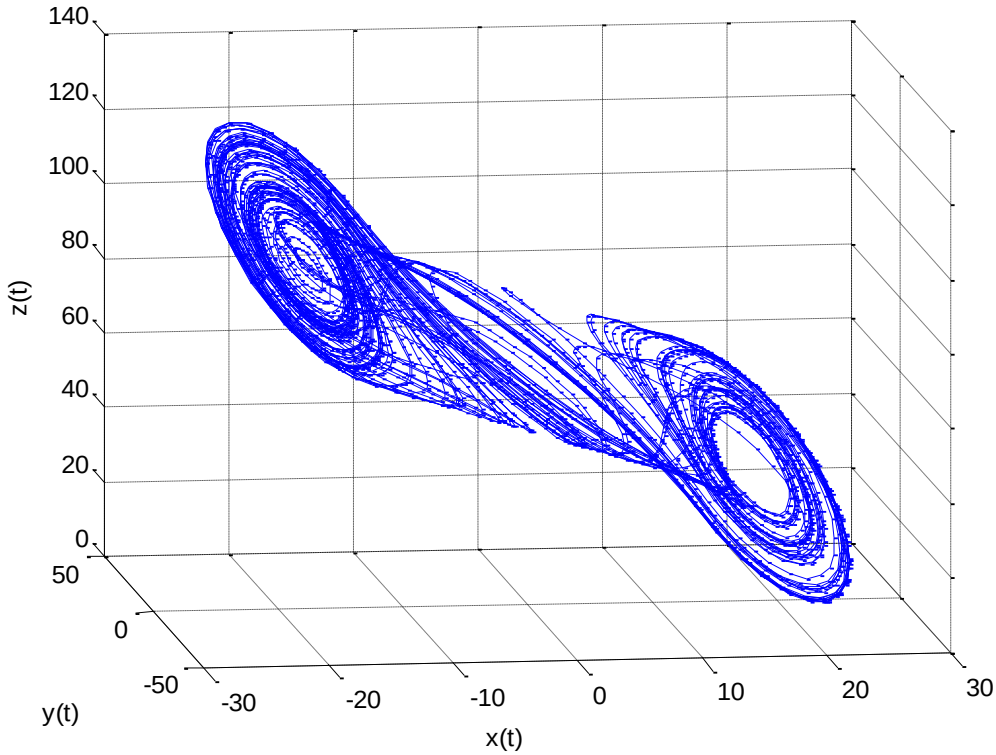

Figure 2.3 : Behavior of Chua's Circuit in three-dimensional space.

2.3 Newton-Leipnik Chaotic System

The system was developed by Leipnik and Newton in 1981. The system has two strange attractor [39]. The system is built by three partial derivatives [40] that shown in Eq 3:

$$\begin{aligned} \dot{x} &= -ax + y + 10yz \\ \dot{y} &= -x - 0.4y + 5xz \\ \dot{z} &= bz - 5xy \end{aligned} \qquad [3]$$

In this equation set, a and b represent constants. $\dot{x}, \dot{y}, \dot{z}$ are partial drivatives as $\dot{x} = \frac{d^{q1}x}{dt^{q1}}, \dot{y} = \frac{d^{q2}y}{dt^{q2}}, \dot{z} = \frac{d^{q3}z}{dt^{q3}}$. The order of the derivatives is determined by q1, q2 and q3 parameters. According to literature searches, systems shows chaotic behavior if a=0.4, b=0.175, q1=q2=q3=α, 0.92<α<1 selected [40]. The alpha variable was selected as α=0.95 in this system. When all these equations (in Eq 3) are solved with the above parameters, the response of the system is as in Figure 2.4:

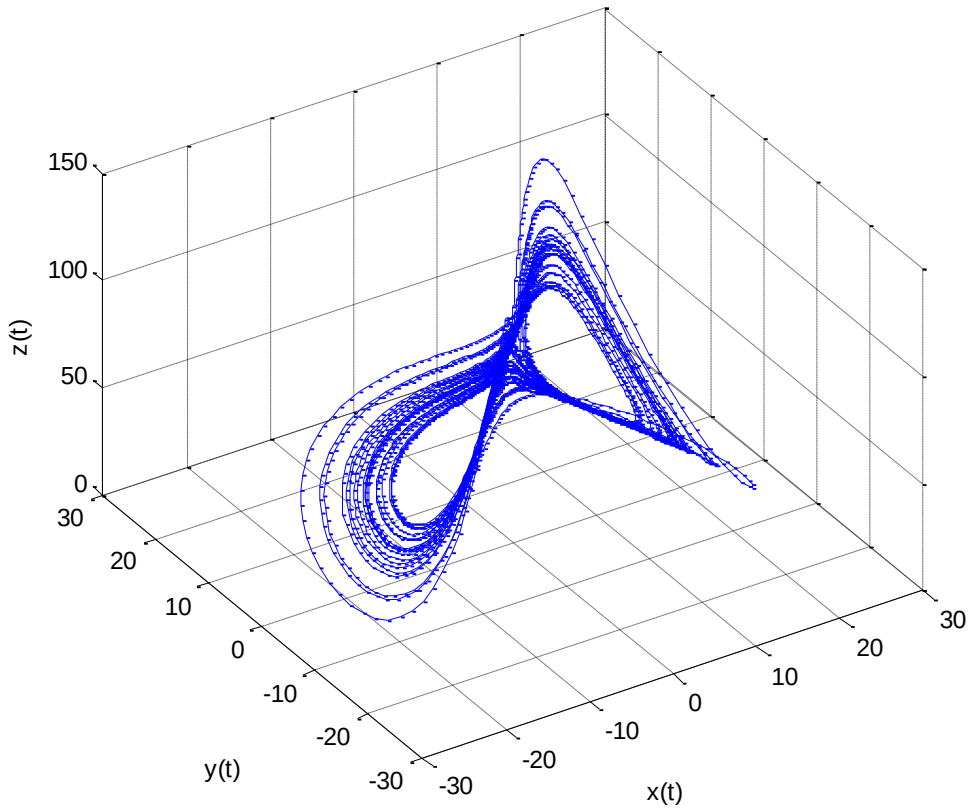

Figure 2.4 : Response of the Newton-Leipnik chaotic system in 3D axis.

2.4 Chen Chaotic System

Developed by Guanrong Chen in 1999. It is defined by three differential equation shown in Eq. 4 [41]:

$$\begin{aligned} \dot{x} &= a(y - x) \\ \dot{y} &= (c - a)x - xz + cy \\ \dot{z} &= xy - bz \end{aligned} \qquad [4]$$

Positive constants are defined by a, b and c while x, y, z are state variables. In many articles and scientific works the constants are selected as; a=35, b=3, and c=28 to obtain chaotic behavior of the system. A solution of the equation set (in Eq.4) creates the graphic shown in Figure 2.5:

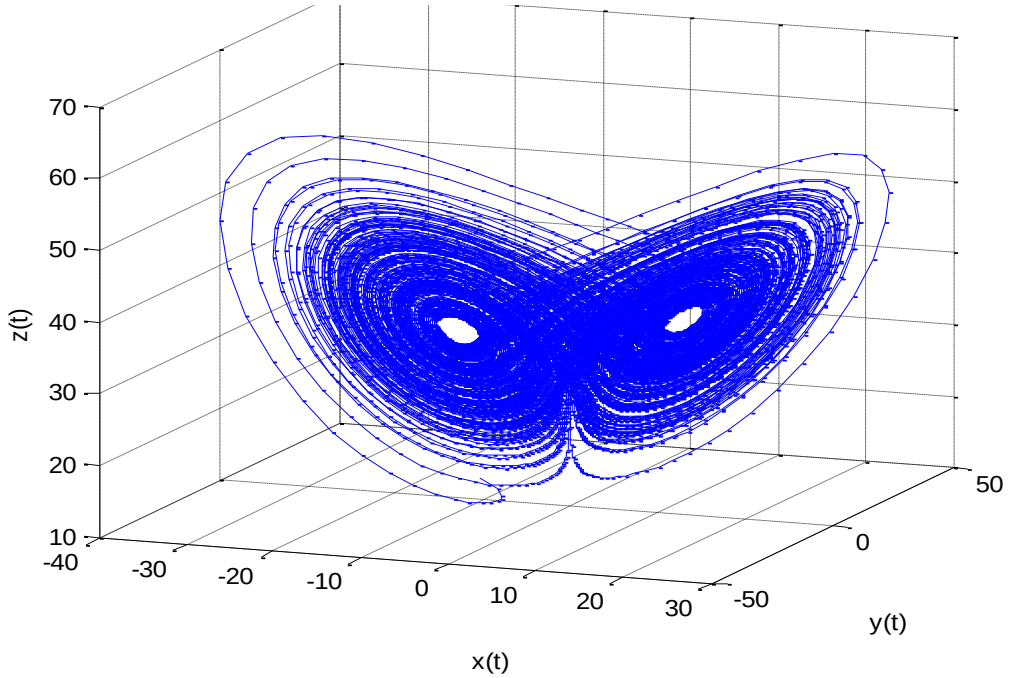

Figure 2.5 : Output of Chen chaotic system in 3D axis.

2.5 Rössler Chaotic System

Rössler Chaotic System is defined three differential equation set as many chaotic systems. It was developed in 1976 by Otto Rössler [42]. The equation set is expressed in Eq. 5:

$$\begin{aligned} \dot{x} &= -y - z \\ \dot{y} &= x - ay \\ \dot{z} &= b + z(x - c) \end{aligned} \qquad [5]$$

x, y, and z show state variables. a, b and c define positive constants. According to common works on literature, system shows chaotic behavior if positive constant are selected as; a=0.5, b=0.2 and c=10 [43]. The simulation output of the system is shown below in Figure 2.6:

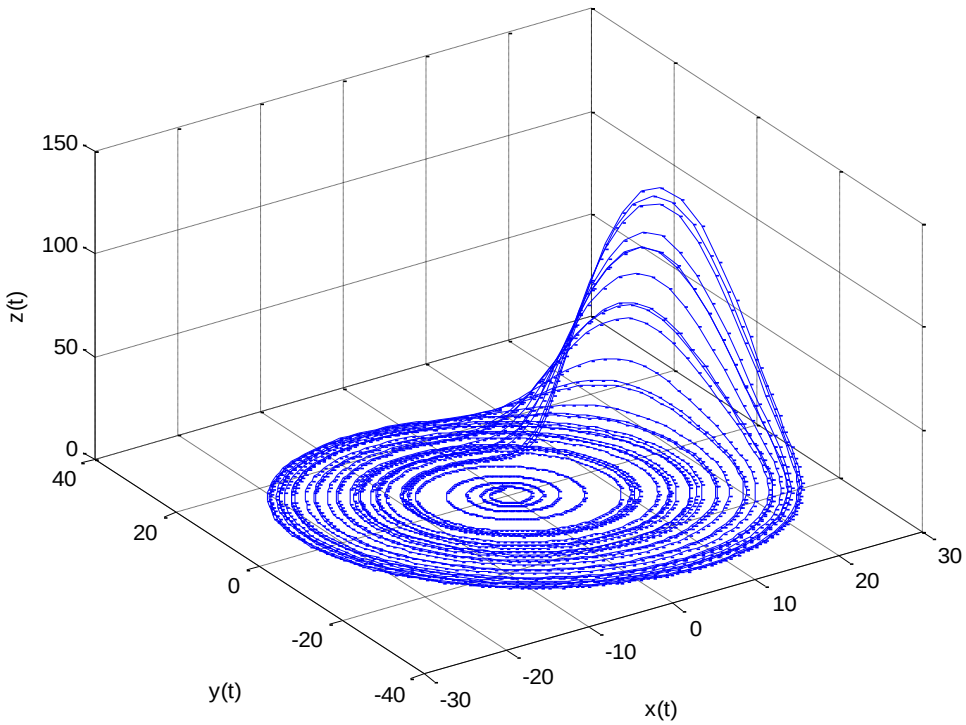

Figure 2.6 : Simulation result of Rössler chaotic system in 3D.

3. MATERIALS AND METHODS

In this chapter, fundamentals and details of the system are explained into five sections. These are; Construction of the delta robot blender system, Modelling of the system with fluid material and DC motor blender, Chaotic drive of blender DC motor in the delta robot via partitioned robust control, Chaotic drive of blender DC motor in the delta robot via sliding mode control, Implementation of the chaotic blending system by embedded system board.

3.1 Construction of the Delta Robot Blender System

At this stage; the mechanical, electrical and software design of the chaotic system-based delta robot robust liquid blender system are explained. The Delta robot is a parallel manipulator mechanism which consists three arms. These three arms are connected by universal joints on the base. The most important feature of the delta robot is that the mobile platform only makes movements in three axes and does not allow any rotational movement. Thus, it can be guaranteed that the direction of the blender shaft changes always the vertical axis. The design of the delta robot blender was handled via SolidWorks software shown in Figure 3.1. The completed construction of the delta robot is shown in Figure 1.1 at Introduction chapter.

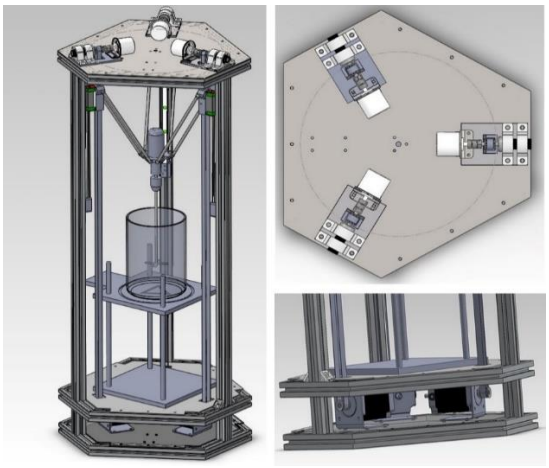

Figure 3.1 : Design of the delta robot (a) side view, (b) top view, (c) bottom view.

3.1.1 Mechanical design of the delta robot

The materials that the delta robot contains are listed below:

- 3 stepper motors (NEMA23) with encoder to drive the arms of the robot,
- 3 belts to move the system in x, y, z direction,
- 3 switches,
- A 350 rpm DC motor mounted to blending shaft,
- 30:1 metal gearbox mounted between shaft and DC motor,
- Encoder mounted to the DC motor

The three stepper motors are mounted at a 120° angle to form (as an equilateral triangle) on the robot top plate, suitable for delta robot construction. These three motors move to the belts which are guided in the vertical axis (z axis) as seen in Figure 3.2. Thus, the circular motion of the stepper motors becomes a linear motion. In the bottom plate of the robot, three 400 step encoders connected to end of the belts (top of the robot). The switches at the top of the system stops the movement of stepper motors at the end of the rail. These switches also prevent step motors stuck at the top.

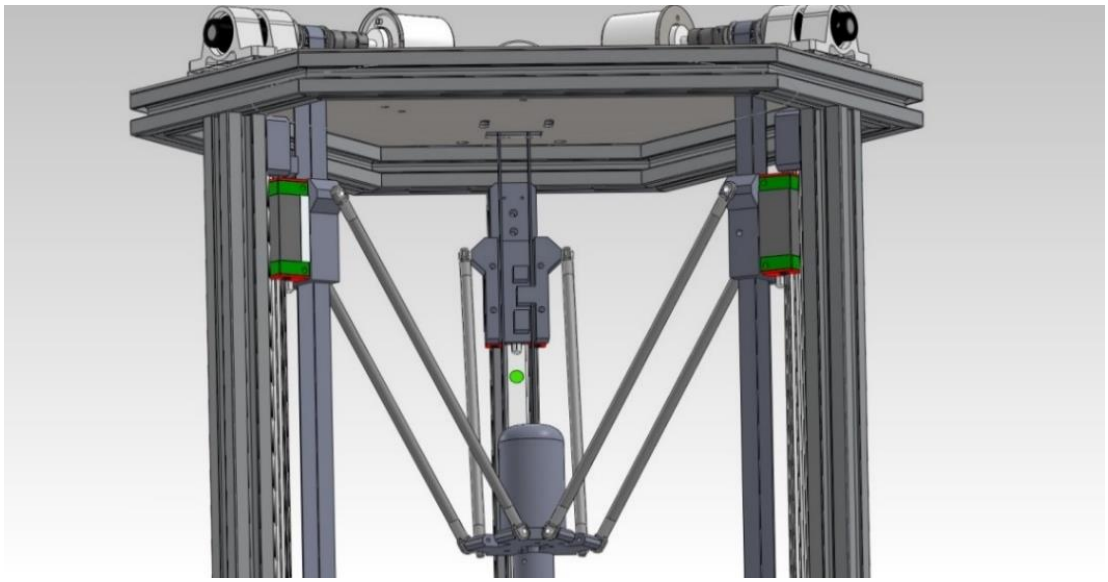

Figure 3.2 : Position of the blender.

The movement of the center point (which is at the intersection of the three arms.) of the robot in the horizontal axis is achieved by positioning the plastic wedges at different heights with the stepper motors moving independently of each other. For vertical axis movements, each stepper motor moves up or down by an equal number of steps. The robot moves smoothly on three axes by using these two types of motion combinations defined in the horizontal and vertical axes.

A DC motor is positioned to perform the blending operation at the intersection point of three arms. A gearbox of 30:1 is connected to the end of the DC motor to increase the rotational force (torque). This gearbox was helps blending of liquids that have higher density and stickiness. A mixer shaft is mounted at the output end of the gearbox. Mixing is carried out with the propellers added to this shaft end, shown in Figure 3.3.

Figure 3.3 : Different size of propellers.

3.1.2 Electrical design of the delta robot

All components in the delta robot are driven by two Arduino Mega 2650 microcontroller platforms (one master, one slave position). These components are; three stepper motors, a DC motor and all encoders. In addition, all stepper motors and DC motor have their own individual motor driver cards. The electrical design scheme of the delta robot is shown in Figure 3.4.

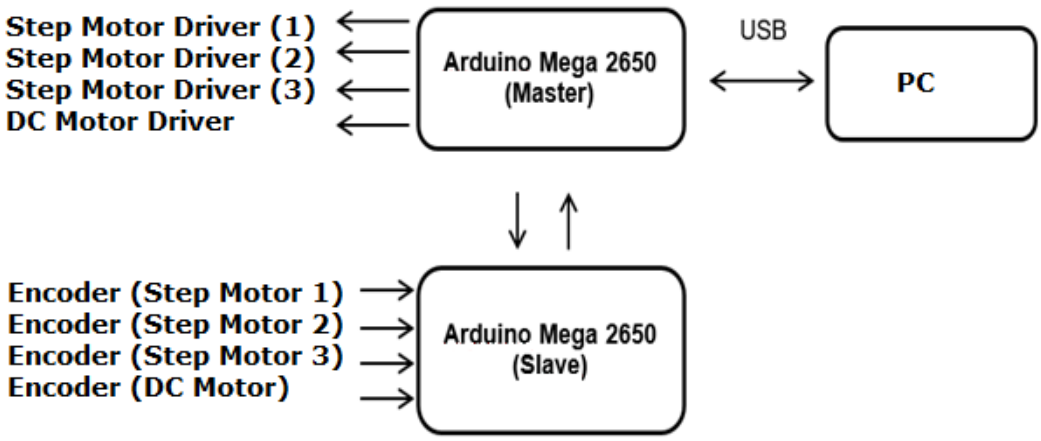

Figure 3.4 : Electrical Design Scheme of Delta Robot.

Single Arduino Mega 2650 microcontroller platform is insufficient for reading the speed information from the four encoders, data transfer to computer via USB and data transmission to motor drives. To overcome this problem, a second Aduino Mega 2650 microcontroller was added as slave card to fulfill the task of reading encoders on the system. The connection between the two microcontrollers is provided by the serial port interface. The real photo of the inside of the electrical control box is shown in Figure 3.5.

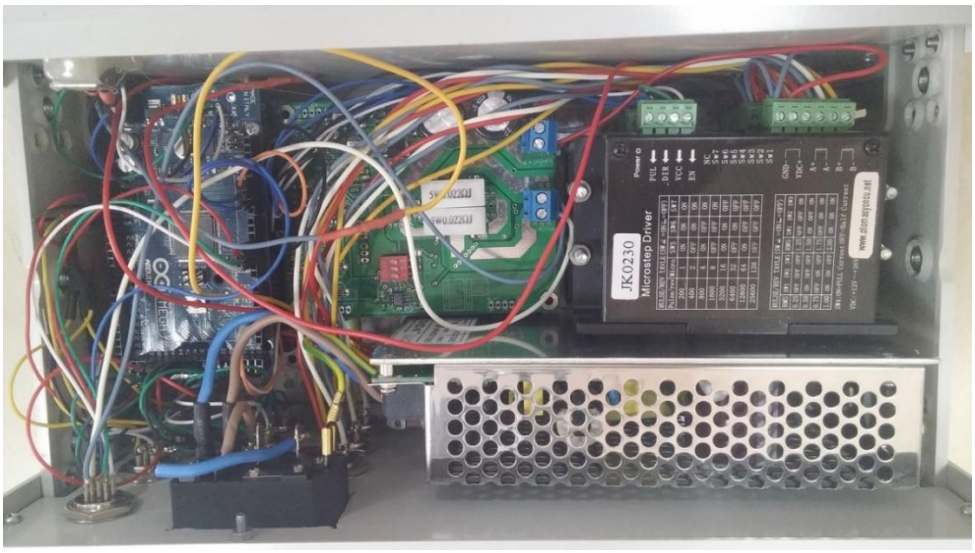

Figure 3.5: Inside of the electrical control box.

The working principle of the system is explained with following steps:

1. Instantaneous coordinate and speed information is calculated according to chaotic systems by MATLAB software. They are transmitted to the micro controller via USB connection.

2. Control of the motors is ensured the microcontroller which transmits the information come from MATLAB to the motor drivers.
3. The instantaneous speed information of the motors is read continuously by the slave microcontroller.
4. The speed information is transferred to the master microcontroller.
5. After the necessary calculations are made in the master microcontroller, speed information is sent back to the PC and MATLAB software.
6. The whole steps at 1-5 continue infinitely.

The 3D coordinate and speed information calculated by the chaotic control system (run in MATLAB platform) is transferred to the master micro controller via virtual the serial port established by the USB line. The baud rate value is set to 9600 in the virtual serial port connection created for this transfer. In addition, asynchronous connection method is used. After the connection between the PC and the master microcontroller is established, communication is provided by the serial port and character transmission method.

The master microcontroller translates the speed and position information (coming from MATLAB) from string type to integer type. The obtained values are transmitted to the motor drivers. The PWM amplitude changes between 0 and 255 to regulate speed of the DC motor in the blending task. On the other hand, the 3D Cartesian coordinate data from the PC is used to calculated in kinematic analysis of the system. After that the necessary step commands are sent to each stepper motor driver individually to implement the desired movement.

The speed information obtained after sending the commands to the motors is read by the encoder mounted to the DC motor and sent to the controller. The speed information from the DC motor encoder is also used as a direct input in the chaotic system equations described in section 3.3.

3.1.3 Software Design of the Delta Robot

To obtain practical and visualize usage of the delta robot blender, a graphical user interface (GUI) was created in the MATLAB platform as shown in Figure 3.6.

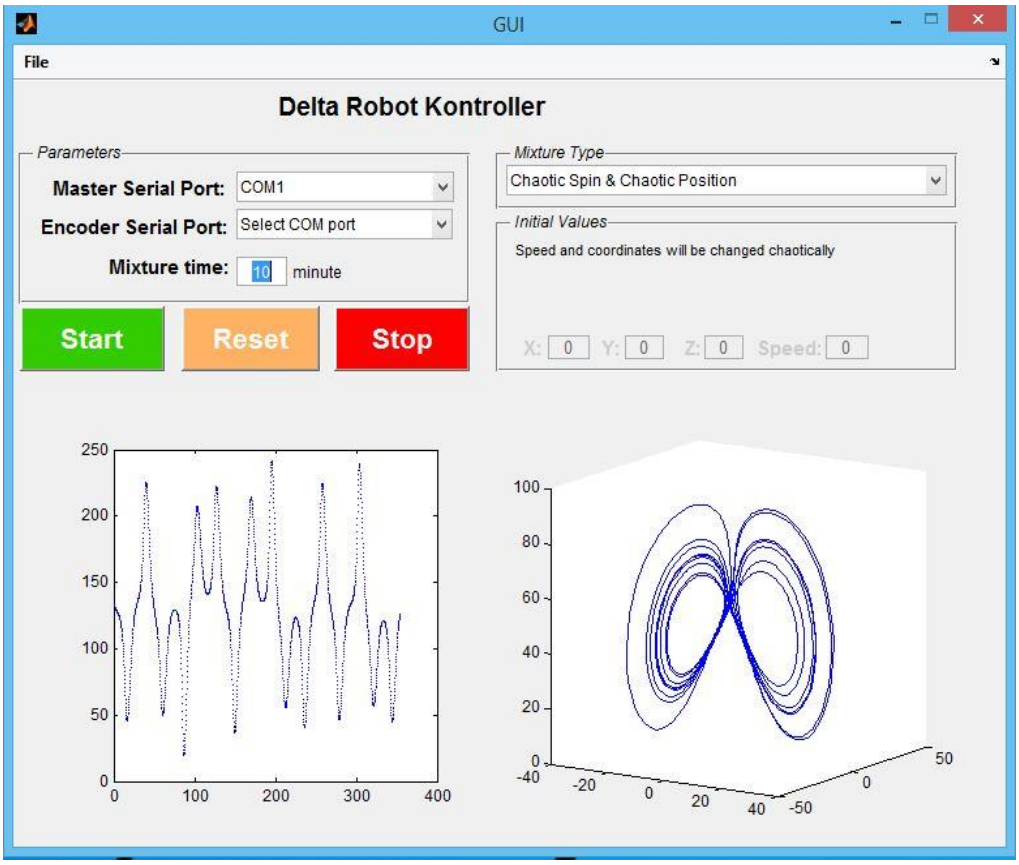

Figure 3.6 : Graphical User Interface for Delta Robot Blender.

While preparing the interface, the care has been taken to keep the usage as simple and practical as possible. Users can select the serial port of the master and slave Arduino cards. After that, mixing time and mixing methods are selected. There are four different blending methods for use in the thesis:

1. Constant speed and constant trajectory
2. Chaotic speed and constant trajectory
3. Constant speed and chaotic trajectory
4. Chaotic speed and chaotic trajectory

The details of the blending methods are explained in “Analyses and Results” section. The user must choose one of these four different methods. After all settings are selected, the "start" button is pressed to begin using the delta robot blender. During operation, the robot can be monitored online with two graphs which are; blending speed and trajectory. Users can restore the robot to the starting coordinates with the

"reset" button. The "Stop" button disconnects the serial USB connection between the robot controller Arduino and the PC.

In addition, a separate option has been added to allow users to manually use the robot (Figure 3.7). At this point, the user can position the propeller of the robot to the desired coordinates and / or the motor shaft of the blender can be rotated at the desired speed.

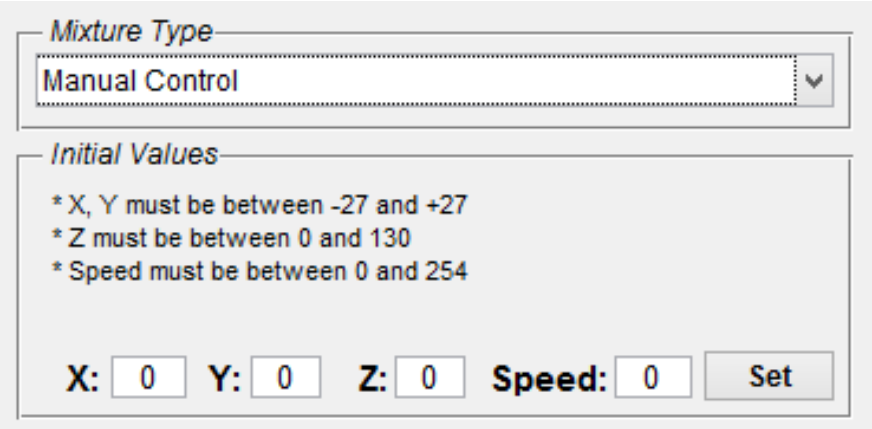

Figure 3.7 : Manual control Options of the Delta Robot Blender.

3.2 Modelling of the System with Fluid Material and DC Motor Blender

In this section, a 3-axis chaotic motion of a chaotic system-based robot and a mathematical model of the combination of DC motor and blending material are found. The mathematical model was developed in two stages. In the first stage, the chaotic system-based delta robot is matched to the state variables of each axis chaotic system. Thus, the orbit the robot will follow in 3-axis space is determined as the orbit of the referenced chaotic system. In the second stage, the design for chaotic driving of the DC motor connected to the shaft of the robot and performing the blending process is considered. Two different chaotic systems that are used in the system have been identified. The five chaotic systems that are explained at "2. Literature Review" section, are simulated one by one in MATLAB platform with reference coefficients. Outputs of these systems have been analyzed in terms of quantity and quality.

3.2.1 Observational analyses

During the determination of the method to be applied for blending, an analysis based on both qualitative observations and numerical calculations was applied. The most important qualitative factors are; the orbit to scan the most points in the beaker, to reach the sides of the beaker, and to distribute the beaker uniformly throughout each

zone. It is aimed to obtain a homogeneous mixture with a shorter time interval and less energy.

It can be easily observed that the Rössler and Chua systems are not homogeneously distributed when the five systems given in the Literature Review are examined. The trajectory in the Rössler system forms between the two corners of the Chua system as it converges at the bottom and one edge of the beaker. In Chen, Lorenz and Newton-Leipnik chaotic systems, it was observed that the trajectory was more homogeneously distributed.

On the other hand, the trajectory obtained from the Chen and Lorenz systems was more concentrated in the center of the beaker. In the Newton-Leipnik system the trajectory reached not only center of the beaker but also edges of beaker. Considering all these results, the use of the Newton-Leipnik system was considered suitable according to observational analyses. This decision is also supported by numerical calculations which will be explained in the following section.

3.2.2 Numerical analyses

The output of each system was created by making 40000 iterations. Obtained trajectories were scaled proportionally to the dimensions of the beaker. These values are applied between -30 mm and + 30 mm for x and y axes and between 0 mm and 130 mm for z axis. The scatter of the trajectory in the beaker in eight different zones were calculated. These calculations will be explained in section 3.2.2.1 and 3.2.2.2.

3.2.2.1 Distribution of the trajectory points in the beaker

To determine the density of the created trajectories inside the beaker, the blending beaker was divided into 8 different zones. Each area was created by taking the midpoint of the three-axis as reference point. The illustration of region is shown in

Figure 3.8. Also, their coordinates are presented in Table 3.1.

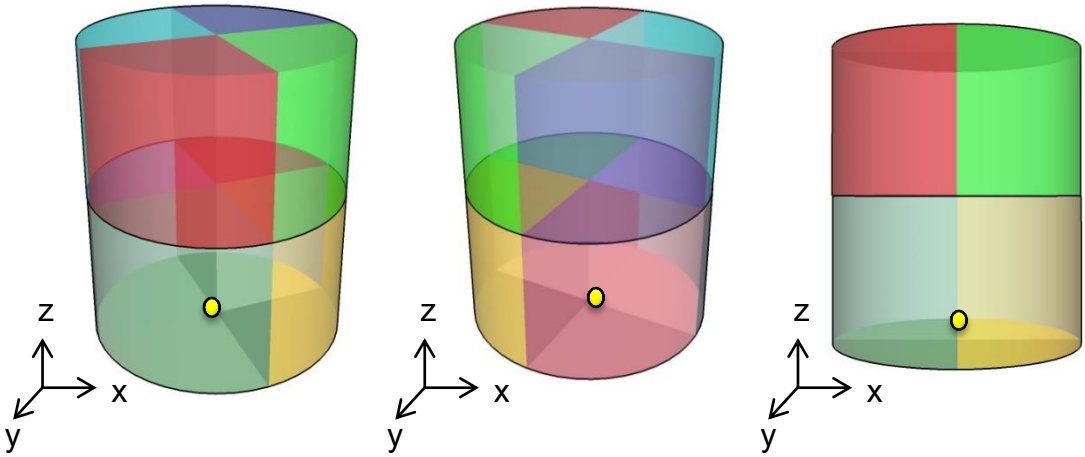

Figure 3.8 : Display of the technical drawing of the beaker separated by the divisions from different angles. (The regions are labeled with different colors for a clearer understanding.) The yellow dot at the bottom of the beaker indicates the center of the coordinate system (0,0,0).

Table 3.1 : The coordinate value of the areas.

Region	X (mm)	Y (mm)	Z (mm)
Region 1	-30-0	-30-0	0-65
Region 2	0-30	-30-0	0-65
Region 3	-30-0	0-30	0-65
Region 4	0-30	0-30	0-65
Region 5	-30-0	-30-0	65-130
Region 6	0-30	-30-0	65-130
Region 7	-30-0	0-30	65-130
Region 8	0-30	0-30	65-130

The set of points of the five chaotic systems are classified. The classification results are given in Table 3.2.

Table 3.2 : Distribution of the trajectory points in the beaker.

Region	Lorenz	Chua	Newton-Leipnik	Chen	Rössler
Region 1:	31%	2%	9%	27%	20%
Region 2:	2%	19%	10%	1%	23%
Region 3:	2%	3%	12%	1%	36%
Region 4:	19%	18%	8%	35%	20%
Region 5:	26%	28%	19%	15%	0%
Region 6:	5%	2%	8%	1%	0%
Region 7:	2%	26%	16%	2%	0%
Region 8:	13%	2%	18%	18%	1%
Total:	100%	100%	100%	100%	100%

In ideal conditions, the distribution of the most homogeneous density points for the eight regions is 100/8=12.5% for each region. As can be seen from the Table 3.2., the system that covers the area more homogeneously in the beaker is the Newton-Leipnik system. Particularly the Rössler and Chua systems can be easily observed in a certain part of the beaker. The Lorenz and Chen methods covers the beaker with a traverse trajectory.

3.2.2.2 Scatter of the trajectory points in the beaker

Euclidean distances between the center of trajectory and all points in the trajectory were calculated one by one to determine how far the generated trajectory points are scattered in the beaker. These calculated distances were cumulatively summed to determine the total distance from the center of the points. These values give us information about how much the observed trajectory is distributed in the volume of beaker. The distribution values calculated for the five systems are given in Table 3.3.

Table 3.3 : Total scatter of the trajectory points in the beaker.

Chaotic System	**Cumulative distribution (cm)**
Lorenz	2717,70
Chua	3073,65
Newton-Leipnik	2975,41
Chen	2326,86
Rössler	809,69

According to the results in Table 3.3, the most scattering system is the Chua chaotic system. Newton-Leipnik and Lorenz systems are close to each other. The Rössler system has low value because it focuses on one region.

As a result, according to the analysis of the distribution and scattering in the baker was evaluated. The Newton-Leipnik system best meets the desired criteria. This result has been proven both by observations and by numerical analyses. As a result, the behavior of the Newton-Leipnik system in the x, y, z coordinates are implemented to the delta robot blender.

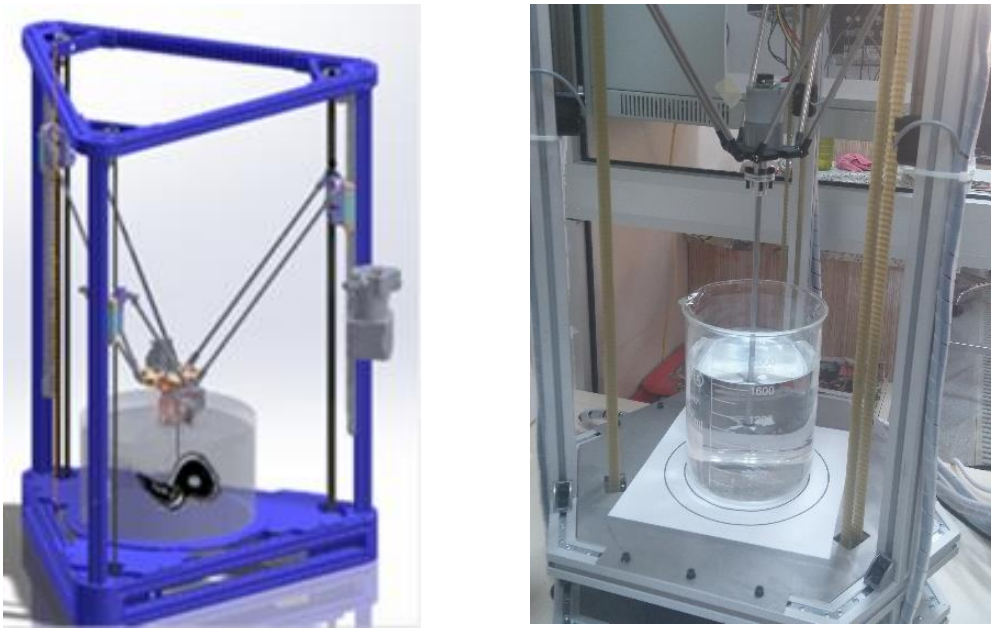

(a) (b)

Figure 3.9 : Figure of delta robot blender's chaotic trajectory (a) illustration, (b) application.

3.3 Chaotic Drive of Blender DC Motor in the Delta Robot via Partitioned Robust Control

The delta robot-based chaotic mixer DC motor system was implemented using real-time simulation environment (Figure 3.6). The mixer robot system and the computerized controller algorithm are operated using the USB interface. The controlling algorithm runs on MATLAB software operated on Microsoft Windows operating system. The block diagram of the delta robot-based chaotic mixer system and its implementation are given in Figure 3.4.. The chaotic control signal which is converted to the Pulse Width Modulation (PWM) signal is applied to the DC motor.

For the chaotic driving of the blender DC motor via Partitioned Robust Control (PRC), a mathematical model of the system was found. The canonical form displays for the chaotic DC motor connected to the robot is shown by the dynamic nonlinear structure in the feedback line. A linear time-invariant single-input system can be defined as $\dot{\hat{\boldsymbol{x}}} = \widehat{\boldsymbol{A}}\boldsymbol{x} + \widehat{\boldsymbol{b}}u$ with state variables. The manageability of such a system requires that manageability matrix $[\widehat{\boldsymbol{b}} \dots \dots \widehat{\boldsymbol{A}}\widehat{\boldsymbol{b}} \dots \dots \widehat{\boldsymbol{A}}^{\boldsymbol{n-1}}\widehat{\boldsymbol{b}}]$ has order of "n". When this condition is satisfied, the state variables of the manageable system can be written as the linear transformation of variables $\widehat{\boldsymbol{x}} =: \boldsymbol{Tx}$, the manageable canonical form $\dot{\boldsymbol{x}} = \boldsymbol{Ax} + \boldsymbol{b}u$

$$\begin{bmatrix} \dot{x}_1 \\ \dot{x}_2 \\ \vdots \\ \dot{x}_{n-1} \\ \dot{x}_n \end{bmatrix} = \begin{bmatrix} 0 & 1 & \cdots & 0 & 0 \\ 0 & 0 & 1 & \cdots & 0 \\ \vdots & \ddots & \ddots & \ddots & \vdots \\ 0 & 0 & 0 & 0 & 1 \\ -a_1 & -a_2 & \cdots & \cdots & -a_n \end{bmatrix} \begin{bmatrix} x_1 \\ x_2 \\ \vdots \\ x_{n-1} \\ x_n \end{bmatrix} + \begin{bmatrix} 0 \\ 0 \\ \vdots \\ 0 \\ 1 \end{bmatrix} u \qquad [6]$$

In this equation, u is input signal, old $\widehat{\boldsymbol{x}} =: [\hat{x}_1, \hat{x}_2, \dots \dots . . \hat{x}_n,]^T$ and new $\boldsymbol{x} =: [x_1, x_2, \dots \dots . . x_n,]^T$ state variable vectors before and after transform. Here, $\boldsymbol{A} = \boldsymbol{T^{-1}}\widehat{\boldsymbol{A}}\boldsymbol{T}$ matrix and $\boldsymbol{b} = \boldsymbol{T^{-1}}\widehat{\boldsymbol{b}}$ vector are calculated by **T** (transform matrix).

The basic criterion for chaotic drive of the DC motor is energy consumption. For this criterion, the chaotic systems described in Literature Review section (Newton, Lorenz, Chua, Rössler, Chen) were implemented to the mixer DC motor. These systems are run in the mixture compound and the instantaneous power measurements are measured with a multimeter connected to the computer. The instantaneous power consumption

of the DC motor shown in Figure 3.10, while the average and total power consumption is shown in Figure 3.11. In all these systems, it has been determined that the least energy consumption is in the Chua chaotic system. Therefore, the system to be applied to the blender DC motor is determined as Chua chaotic system.

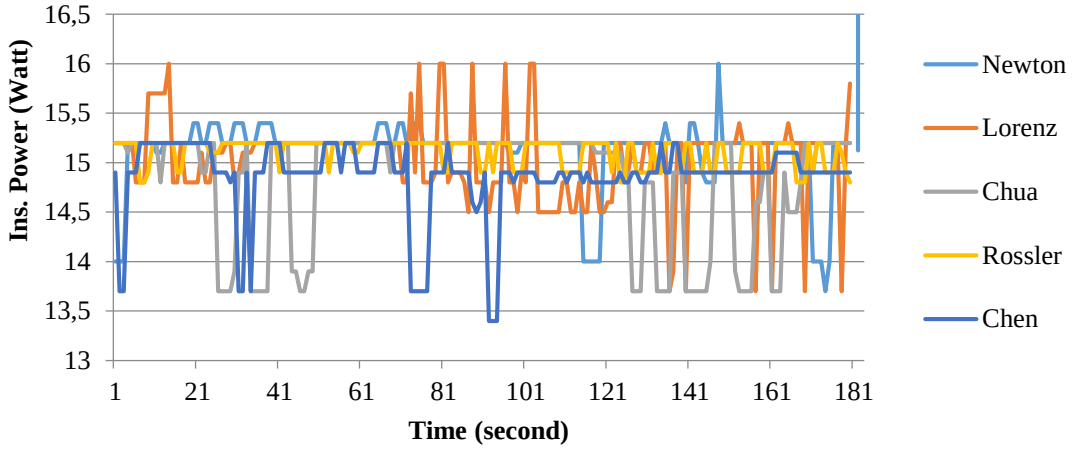

Figure 3.10 : Instantaneous power consumption values of chaotic systems applied to DC motor.

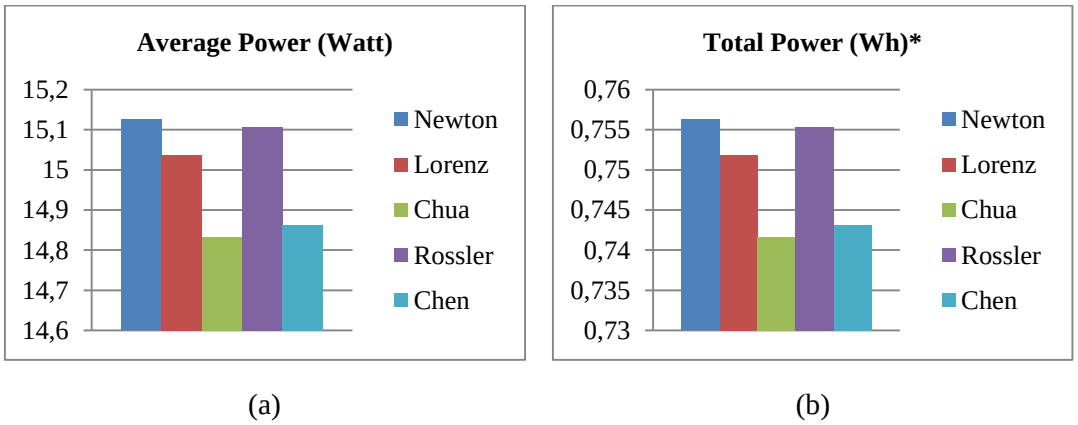

(a) (b)

Figure 3.11 : (a) The average power consumption of the chaotic systems applied to the DC motor (b) the total electric energy consumption. (* Energy (Wh) is calculated by multiplying between average power and time.)

The Chua chaotic system has also used from the previous works in publications [2]. A reference DC motor is chaotized by integrating the encoder feedback of the motor into the Chua chaotic system and the success of the achieved system is shown in the model [2]. The equations of the Chua chaotic system used in the system is as follows:

$$\dot{x} = \alpha(y - x - f(x))$$
$$\dot{y} = x - y + z \qquad [7]$$
$$\dot{z} = -\beta y$$
$$f(x) = m_0 x + \frac{1}{2}(m_1 - m_0)[|x+1| - |x-1|]$$

In the equation above, f(x) is a partial linear function contains two lines with slope $m_0 = -0.68$ and $m_1 = -1.27$. $\alpha > 0$, $\beta > 0$ are constants. A dynamic non-linear feedback is formed to ensure that the DC motor connected to the robot shaft behaves chaotically. To write the controllable linear system with the reference chaotic system, $x_n = x,\ x_{n+1} = y,\ x_{n+2} = z$. The dynamic state feedback control signal is $u = a_1 x_1 + \cdots a_{n-1} x_{n-1} - (\alpha - a_n) x_n + \alpha[x_{n+1} - F(x_n)] + \varepsilon(x_1, \dots, x_n)$. To make the system asymptotically stable in the Lyapunov sense, the terms $\varepsilon(x_1, \dots, x_n)$ are added to each state variable with small amplitude, and the chaotic behavior of the system is preserved.

$$\begin{bmatrix} \dot{x}_1 \\ \dot{x}_2 \\ \vdots \\ \dot{x}_{n-1} \\ \dot{x}_n \\ \dot{x}_{n+1} \\ \dot{x}_{n+2} \end{bmatrix} = \begin{bmatrix} 0 & 1 & 0 & \cdots & 0 & 0 & 0 \\ 0 & 0 & 1 & \cdots & 0 & 0 & 0 \\ \vdots & \vdots & \vdots & \ddots & \vdots & \vdots & \vdots \\ 0 & 0 & 0 & \cdots & 1 & 0 & 0 \\ \varepsilon_1 & \varepsilon_2 & \varepsilon_3 & \cdots & -\alpha + \varepsilon_n & \alpha & 0 \\ 0 & 0 & 0 & \cdots & 1 & -1 & 1 \\ 0 & 0 & 0 & \cdots & 0 & -\beta & 0 \end{bmatrix} \begin{bmatrix} x_1 \\ x_2 \\ \vdots \\ x_{n-1} \\ x_n \\ x_{n+1} \\ x_{n+2} \end{bmatrix} + \begin{bmatrix} 0 \\ 0 \\ \vdots \\ 0 \\ -\alpha F(x_n) \\ 0 \\ 0 \end{bmatrix} \qquad [8]$$

$$\dot{x_n} = -\alpha x_n - [a_1 x_1 + \cdots + a_{n-1} x_{n-1} - (\alpha - a_n) x_n - u]$$
$$= -\alpha x_n + \alpha[x_{n+1} - F(x_n)] + \varepsilon(x_1, \dots, x_n)$$
$$\dot{x}_{n+1} = x_n - x_{n+1} + x_{n+2} \qquad [9]$$
$$\dot{x}_{n+2} = -\beta x_{n+1}$$

The model of these chaotic system is presented in Figure 3.12.

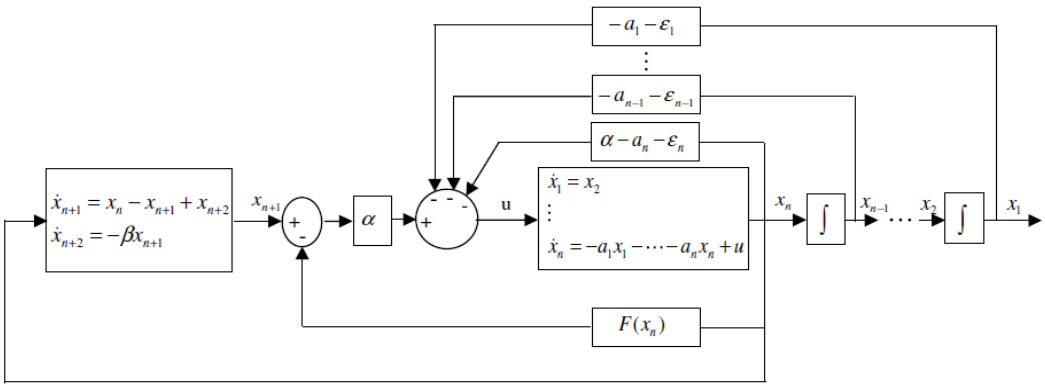

Figure 3.12 : Block diagram of chaotic linear time invariant manageable system [2].

In this model (shown in Figure 3.12.), $\dot{x} = -a_m x + b_m u$ represents the DC motor rotation speed (rpm). The model parameters are found using the MATLAB system with rotation speed values which is measured by the encoder attached to DC motor. The resulting model is calculated from the dynamic linear system structure with first order time delay. A typical process model is represented by three Laplace parameters in the form of a complex number of planes $H(s) = \frac{K}{1+Ts} e^{-Ls}$. In this model, T shows time constant, L shows dead time and K shows gain [44]. The maximum DC motor speed is 350 rpm, T = 1.57 seconds. and the dead time is approximately 0 second from experimental data obtained from the DC motor and nanocomposite compound system. The parameters of this real system have been found by designing a controller that can provide data-dependent online stability through the real system developed [44]. In addition, the system has been verified using the MATLAB system diagnostics tool "ident". After this identification step, K = 16.805 and T = 1.5747 were found. According to these results, $\dot{x} = -a_m x + b_m u$, $a_m = 0.63$, $b_m = 2707/32$ parameters were calculated. The structure and chaotic control signal models for the blender system was generated by the reference Chua chaotic system are given as follows:

$$\dot{x} = -a_m x - (\hat{\alpha} - a_m)x + \hat{\alpha}\big(y - F(x)\big) = -a_m x + b_m u$$

$$\dot{y} = x - y + z$$

$$\dot{z} = -\hat{\beta} y \qquad [10]$$

$$u = \frac{1}{b_m}\left[-(\hat{\alpha} - a_m)x + \hat{\alpha}\big(y - F(x)\big)\right]$$

$$\mathrm{f(x)} = \mathrm{m_0 x} + \frac{1}{2}(\mathrm{m_1} - \mathrm{m_0})[|\mathrm{x}+1| - |\mathrm{x}-1|]$$

In this equation above, $\hat{\alpha} = 9$, $\hat{\beta} = 14.87$, $m_0 = -5/7$ and $m_1 = -8/7$ selected as reference article [38]. The simulation results and actual system application results are shown in Figure 3.13, Figure 3.15 and Figure 3.14.

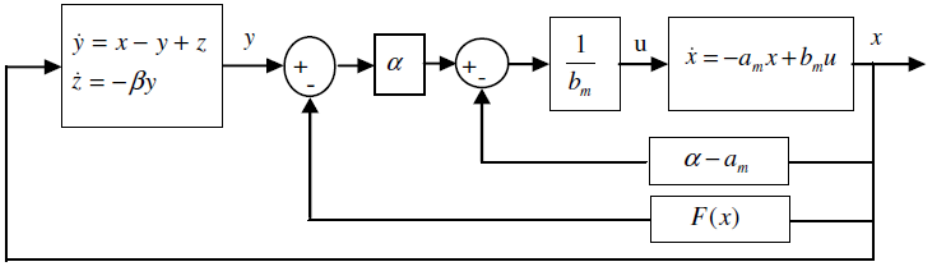

Figure 3.13 : The block diagram of chaotification of DC motor via dynamic state feedback [2].

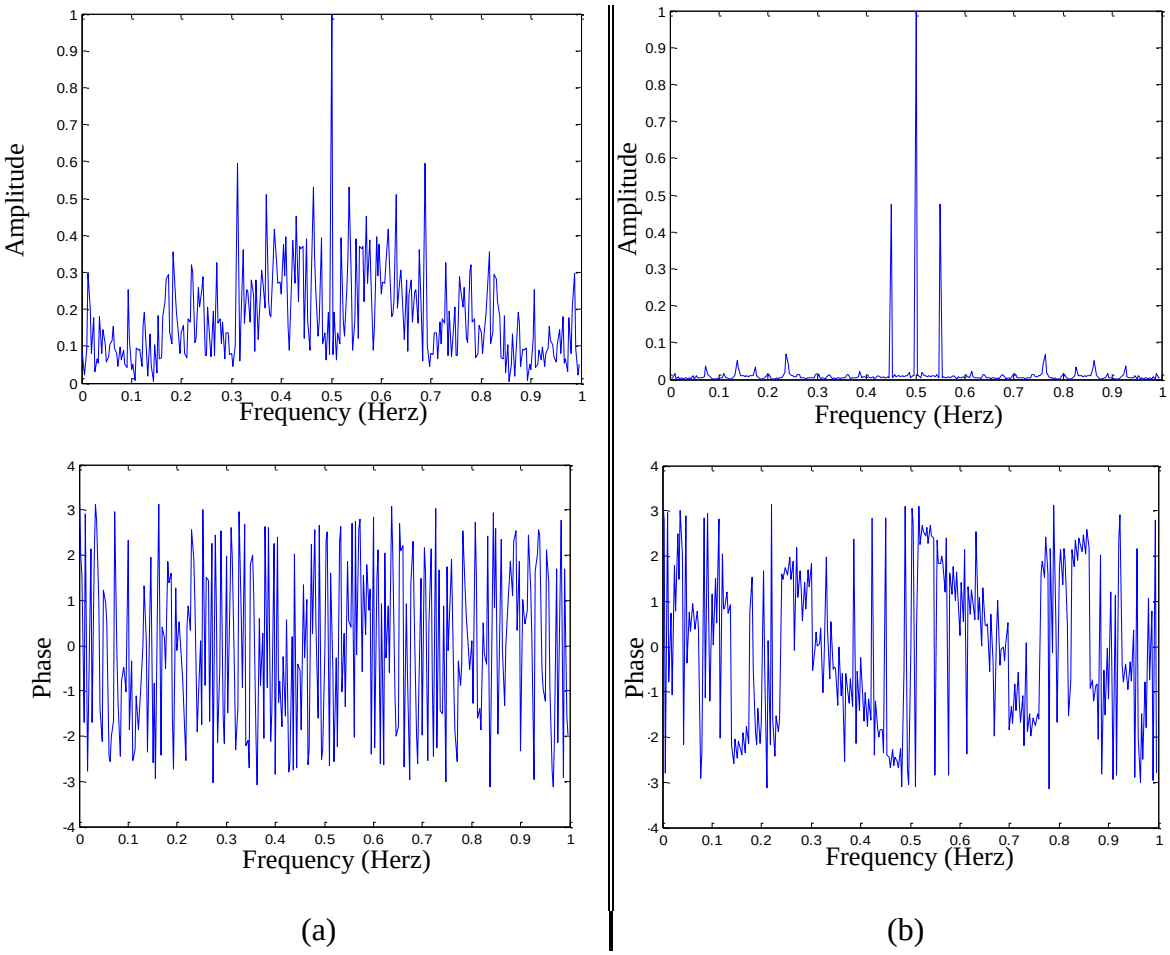

Figure 3.14 : (a) Amplitude and phase spectrum of DC motor driven via chaotic signal. (b) Amplitude and phase spectrum of DC motor driven via periodic signal.

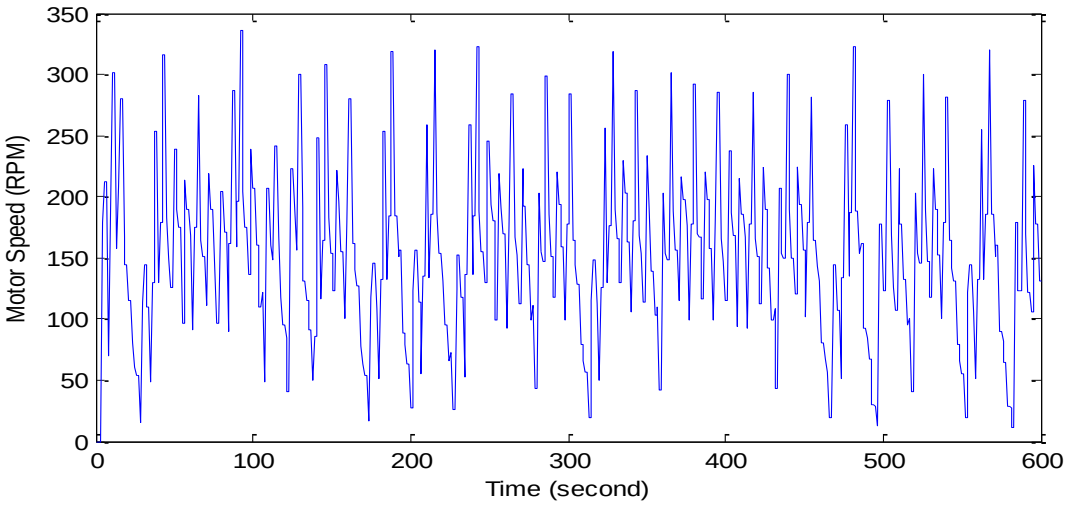

Figure 3.15 : Real-time speed / time graph of the chaotically driven DC motor.

3.4 Chaotic Drive of Blender DC Motor in the Delta Robot via Sliding Mode Control

In this section, model based chaotic methods are applied with sliding mode control (SMC) [45]. The method used involves a dynamic state feedback method to match the system's states with the reference chaotic system. In this method, all the disturbing effects that can be added to the system are accepted as additional input to the noisy system. These inputs are defined as an unknown function that falls within the limits of a known function. The intermittent feedback controller architecture of the SMC method provides robustness against noise and other disturbing effects. Against noise and disturbing effects, the system provides a chaotic behavior in each input range. This method requires a reference chaotic system in normal form. For this reason, the reference chaotic system has been transformed into the normal form. With the obtained controller structure, the delta robot based chaotic mixer system is designed. An n-dimensional, single-input, observable linear system is written as in the following equation:

$$\dot{x} = Ax + b[u + \delta(t, x, u)] \qquad [11]$$

$A\epsilon R^{nxn}$, $b\epsilon R^{n}$, u represent the control input, $\delta(t, x, u)$ represents noise, distortion and other external factors in the system. Assuming that, this linear system is controllable, the given system can be linearly transformed into a normal form with a transformation of $z = Tx$. The normal form resulting from this transformation is shown in equation below:

$$\dot{z} = \begin{bmatrix} 0 & 1 & 0 & \dots & 0 \\ \vdots & \ddots & & & \vdots \\ \vdots & & \ddots & 1 & 0 \\ 0 & \cdots & \cdots & 0 & 1 \\ a_0 & a_1 & \cdots & \cdots & a_{0n-1} \end{bmatrix} z + \begin{bmatrix} 0 \\ 0 \\ \vdots \\ 0 \\ 1 \end{bmatrix} [u + \delta(t, T^{-1}, u)] \qquad [12]$$

In this transform, $\delta(t, T^{-1}, u)$ represents noise, distortion and other external factors in the system. Dynamic feedback rule is defined as:

$$u = -a_0 z_1 - a_1 z_{2\,-} - \cdots - a_{n-2} z_{n-1} - a_{n-1} z_n + \dot{z}_n - \ddot{z}_n + \frac{\partial G_c}{z_1} z_2 + \frac{\partial G_c}{z_2} z_3 + \cdots + \frac{\partial G_c}{z_n} \dot{z}_n + v \qquad [13]$$

Here, $G_C(z_1, z_2, \dots\dots z_n) : R^n \to R^n$ was selected as jerk function of chaotic system in normal form. When the equation given in Eq. (12) is replaced by Eq. (13), the notation in Eq. (14) is obtained:

$$\dot{z} = \begin{bmatrix} 0 & 1 & 0 & \dots & 0 \\ \vdots & \ddots & & & \vdots \\ \vdots & & \ddots & 1 & 0 \\ 0 & \cdots & \cdots & 0 & 1 \\ 0 & \dots & \cdots & \cdots & 0 \end{bmatrix} z + \begin{bmatrix} 0 \\ 0 \\ \vdots \\ 0 \\ 1 \end{bmatrix} [v + \dot{z}_n - \ddot{z}_n + \frac{\partial G_c}{z_1} z_2 + \frac{\partial G_c}{z_2} z_3 + \cdots + \frac{\partial G_c}{z_n} \dot{z}_n + \hat{\delta}(t, z, u)] \qquad [14]$$

Here, v represents control input, $\hat{\delta}(t, z, u)$ represents noise, distortion and other external factors in the system in terms of z and v. New state variable was defined as $\dot{z}_n = z_{n+1}$ and $\ddot{z}_n = \dot{z}_{n+1}$ After that the state model was obtained as:

$$\begin{aligned} \dot{z}_1 &= z_2 \\ \dot{z}_2 &= z_3 \\ &\vdots \\ \dot{z}_n &= z_{n+1} \\ \dot{z}_{n+1} &= \frac{\partial G_c}{z_1} z_2 + \frac{\partial G_c}{z_2} z_3 + \cdots + \frac{\partial G_c}{z_n} \dot{z}_n + v + \hat{\delta}(t, z, u) \end{aligned} \qquad [15]$$

Based on the structure shown above, the DC motor on the delta robot mixer shaft is provided with robust chaotic behavior by the SMC method. The velocity-time graph obtained at n=3 during application and the result of application is shown in Figure 3.16

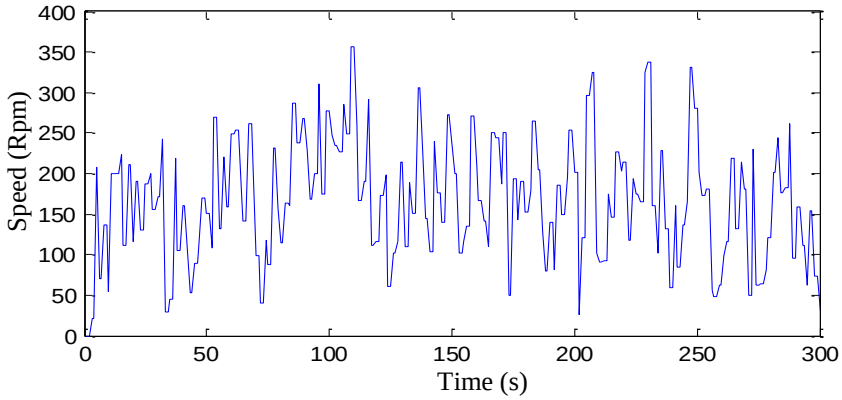

Figure 3.16: Speed-time graph of chaotic drive by SMC method.

After the chaotic usage of SMC for DC motor, the energy consumption measurements of the whole system are made from the mains voltage input, which is the main energy input connection of the system. Energy measurement was handled by measuring instantaneous system power for one minute. The electrical energy consumption comparison with the PRC method and SRC method is shown in Figure 3.17. The values in Figure 3.17 are expressed in terms of kilowatts of energy consumed by the system in one minute. In addition, the energy consumption of the system in standby mode was also measured and indicated in the graphic as "Idle". According to the measurement results, no significant difference in energy consumption was observed between the two methods.

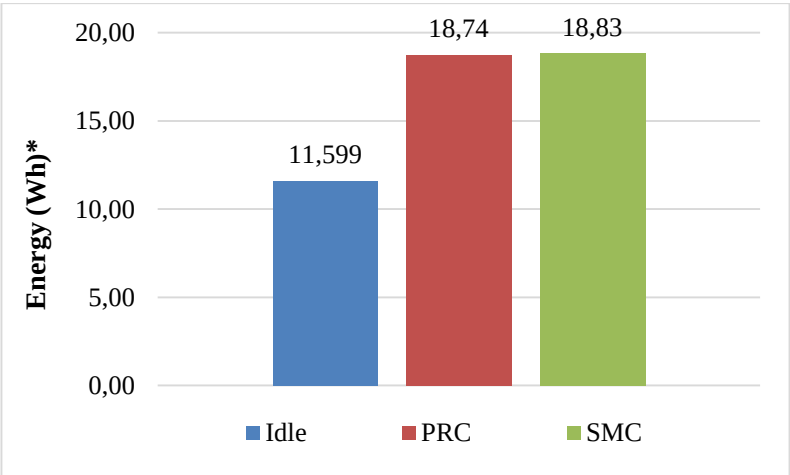

Figure 3.17 : Energy consumptions of Idle state, PRC [2] and SMC [45] methods.
(* Energy (Wh) is calculated by multiplying between average power and time.)

3.5 Implementation of the Chaotic Blending System on Embedded System Board

The main purpose of this section is to ensure that the chaotic-based mixer system operates independently of the PC and can serve as a unique device. The system described in previous sections is controlled by MATLAB software by the PC which is connected to system. In this part of the work, the system has been designed to operate without dependency of PC.

Hardware searches have been done for the operations to be performed by system. The user interaction of the device is provided by one colored touch screen. So far, research has been done on Microchip's PIC series micro controllers, Texas Instruments DSP cards, Arduino platform and Intel Galileo platforms.

Arduino Mega 2650 microcontroller has been chosen as the platform for user control. The following criteria were considered during the selection of the controller:

- Seamless communication with other Arduino microcontrollers in the system.
- Cost effectiveness.
- It is practical to develop interfaces with a touch-screen LCD screen; it has the necessary software libraries.
- Support for application development with C, C ++ or MATLAB languages.

The control system block diagram is designed as shown in Figure 3.18 below:

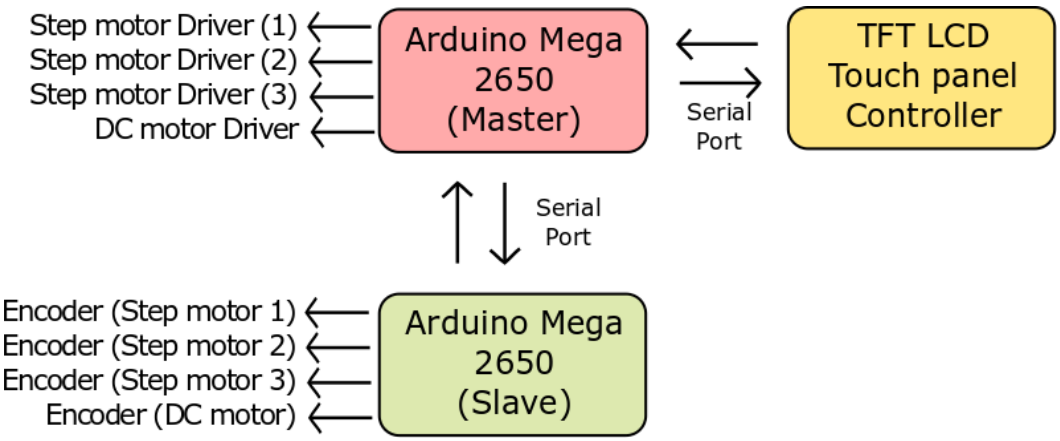

Figure 3.18 : Block diagram of control system.

The ATMEGA microcontroller in the Arduino Mega 2650 platform has three serial port inputs. One is used to establish a USB connection with the computer for virtual serial port, while the other two are left blank for free use. That is why the serial port interface is used for connection to the Arduino Mega 2650 platform in the master position of the system. It is appropriate to use the same model platform to minimize the problems that may occur during connection. The Arduino platform, on the other hand, has a fair price. So, Arduino Mega 2650 is used for user interface design.

It is preferred that the touch screen used in the system is also a convenient but useful model. Users can read the necessary variable settings via the screen and can also enter data into the system via the touch method. The TFT LCD Touch Shield for Arduino Mega model of ITEAD company is used (shown in Figure 3.19). The technical specifications of the display are given in Table 3.4.

Table 3.4 : Specifications of the TFT LCD Touch Shield.

TFT Resolution	240 x 320 pixel
Size	3.2"
Colors	65K
Touch Sensor	Resistive
Back light	LED
Driver IC:	SSD1289
Library Support	Arduino library UTFT support

Figure 3.19 : TFT LCD Touch Shield.

The pin structure of the LCD display is fully compatible with Arduino. D2, D3, D4, D5, D6, D22-D41, D50, D51, D52 and D53 pins are used to operate the display and the circuit.

During the development stage of the interface, the Arduino UTFT library is used. According to this library, the position and color of each element such as all buttons, text, lines to be drawn on the screen are determined one by one. The function block example for placing a button on the screen is given below:

```
myGLCD.clrScr(); //Ekranı temizle
myGLCD.setBackColor(255,51,204); // Arkaplan rengi
myGLCD.setColor(255,51,204); //Başlık Rengi
myGLCD.fillRoundRect (10, 10, 300, 55); // Dikdörtgen doldurma
myGLCD.setColor(255, 255, 255); // Çizgi rengi
myGLCD.drawRoundRect (10, 10, 300, 55); //Sınır çizgisi çiz
myGLCD.print(names1[1], CENTER, 13); //İlk satır başlık
myGLCD.print(names2[1], CENTER, 33); // İkinci satır başlık
```

The touch inputs from the user are continuously read in a "while" loop. The read position information is stored in variables x and y. When the coordinates of the touch input come on the corresponding button, the sub function belonging to that button is called. An example of an algorithm for determining which button belongs to the input from the user input is given below:

```
void ekranOku()
{
  /////// Ana Sayfa ///////
  if ((x>=10) && (x<=300) && page==1)
        {
           if ((y>=10) && (y<=55))
          {
            waitForIt(10, 10, 300, 55);
            sayfa(1);
          }
         if ((y>=70) && (y<=115))
          {
            waitForIt(10, 70, 300, 115);
            sayfa(2);
```

As can be seen from the above code, the pixel belonging to the screen is divided into a grid, and the user input is performed in which region the user belongs. Coordinates that user touched on the touch panel are determined by the bounds of the x and y variables in the “if condition” in the code.

The delta robot based chaotic blender can work in four different scenarios. For this reason, the main page of the user interface consists of four buttons for four different scenarios. The improved Arduino-based control interface is mounted in a panel positioned on the front of the robot to provide an easy user experience. From here it is connected to the main control box shown in Figure 3.5. The position of the interface on the robot and the way it works can be seen from Figure 3.20.

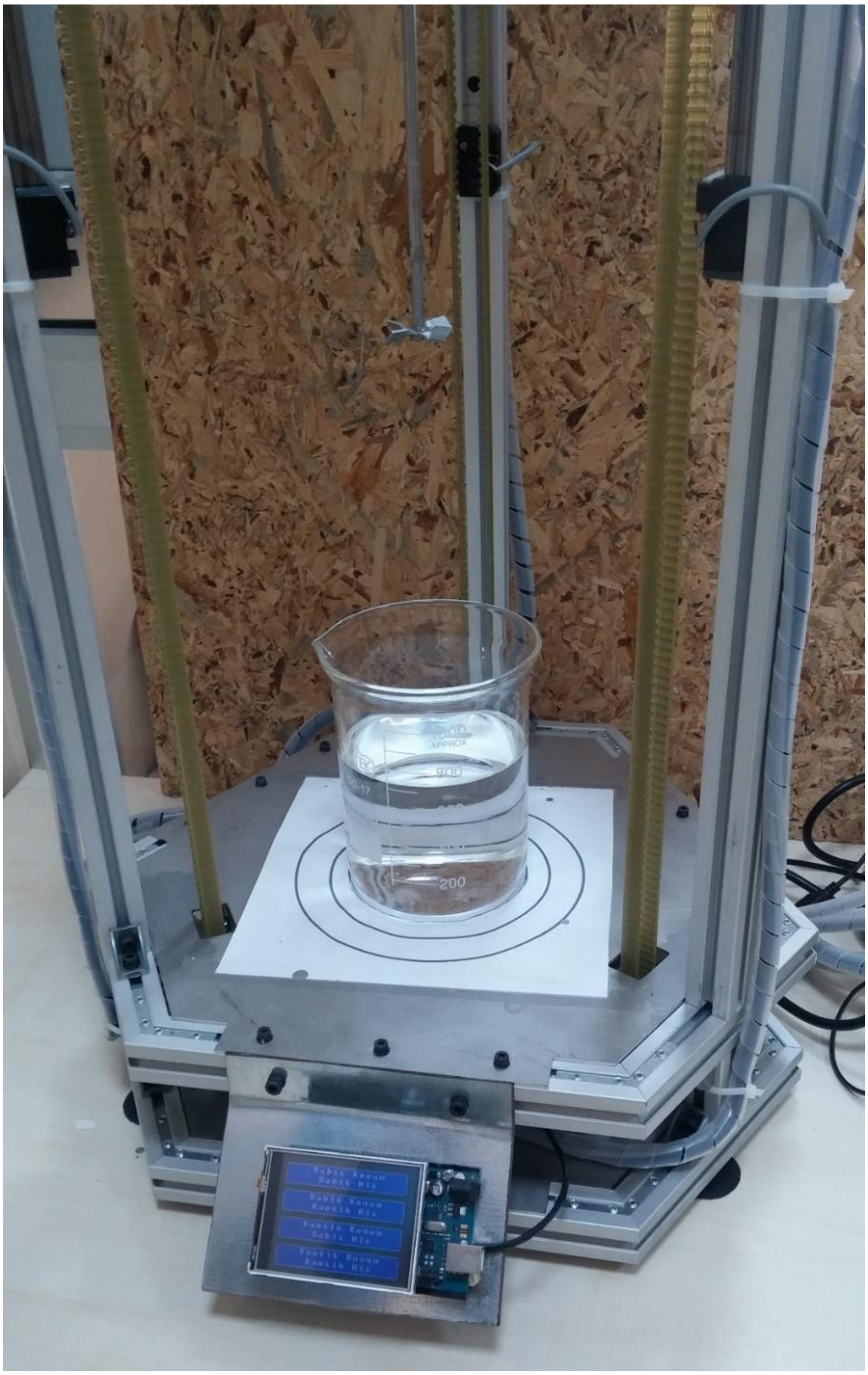

Figure 3.20 : The developed user interface is positioned on the robot.

Users can choose the method they want from the main page. After the desired method is selected, another screen is displayed where the parameters of the relevant method can be seen and changed. For example, the screen shown in Figure 3.21 is designed for the "Constant position, constant speed" method:

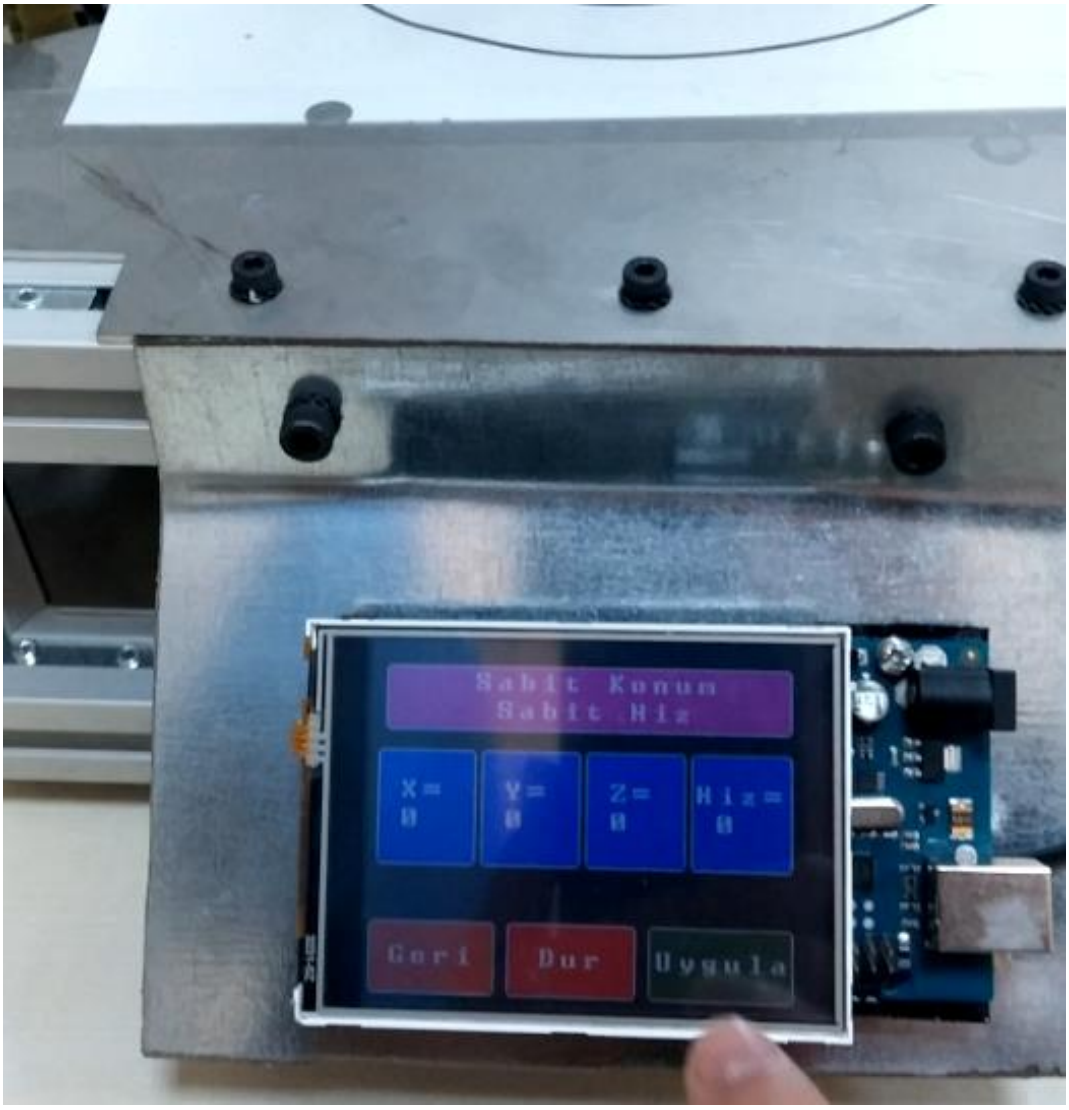

Figure 3.21 : Control page of "Constant position, constant speed" method.

On this screen, users can determine the coordinates and speed of the delta robot-based chaotic blender. When the buttons of the variables are clicked, the virtual keyboard screen opens for data entry in that area Figure 3.22. Through this keyboard, users can input numerical data as they desire. Once all variables have been set, the system can be started with the "Apply-Uygula" button. If users wish, they can return to the main menu with the "back-geri" button.

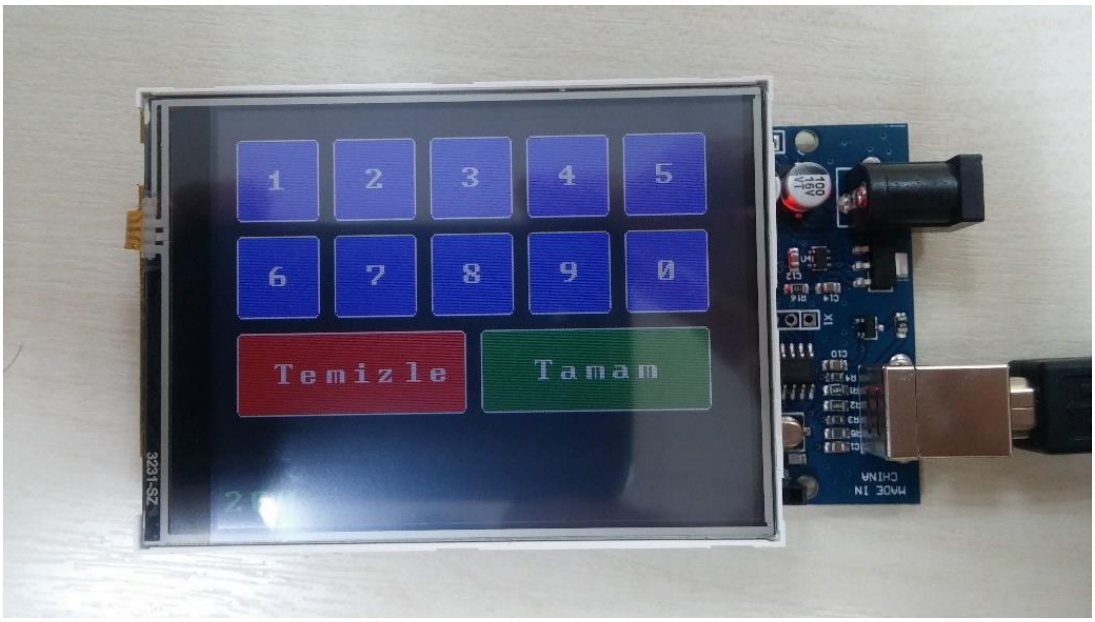

Figure 3.22 : Virtual keyboard designed for data entry.

After the “Apply” button is pressed, Arduino Mega 2650 circuit, which is connected to the screen, communicates with the master Arduino in the system via serial port and sends the necessary motion data. The interface and sub-functions required for the four scenarios of “Constant speed and constant trajectory”, “Chaotic speed and constant trajectory”, “Constant speed and chaotic trajectory” and “Chaotic speed and chaotic trajectory” are completed.

4. ANALYSES AND RESULTS

This section of the thesis is described in the subsections as Blending of polymer nanocomposites, Characterization, Energy consumption analyses. First, mixtures of a nanocomposite material and dye were performed. After that, the performance of the blender was evaluated by homogeneity analysis and microstructural, mechanical and electrical characterization. Finally, that the energy consumption was measured.

4.1 Blending of Polymer Nanocomposites

Blending of polymer nanocomposites were performed separately for four different scenarios which are; “constant speed and constant trajectory”, “constant speed and chaotic trajectory”, “chaotic speed and constant trajectory” and “chaotic speed and chaotic trajectory”.

In the constant speed and constant trajectory scenario, the mixing propeller at the end of the delta robot is set to a fixed position corresponding to the exact center of the mixing chamber. In addition, the propeller is also rotated at a constant full speed. On the other hand, in the constant speed and chaotic trajectory mode, the position of the propeller was changed at half-second intervals to follow the output of the designed chaotic system while the propeller is rotating at a constant speed.

The chaotically rotating propeller is fixed at the center of the beaker when the velocity of the mixer is chaotically changed in the chaotic speed and constant trajectory. In the chaotic speed and chaotic trajectory case, both the rotational speed of the propeller and its coordinates are driven by the chaotic systems.

As a polymer nanocomposite to be mixed in the experiments, graphene material was used. Graphene is an allotrope of carbon atom. It is made up of a special arrangement of carbon atoms. The carbon atom is found in many different materials such as diamonds, graphite, fullerenes, carbon nanotubes. The difference between these materials is different arrangements of carbon atoms. Unlike other carbon-based

structures, atoms are interconnected by a hexagonal (honeycomb) bond in the graphene structure [46; 47]. This structure is shown in Figure 4.1.

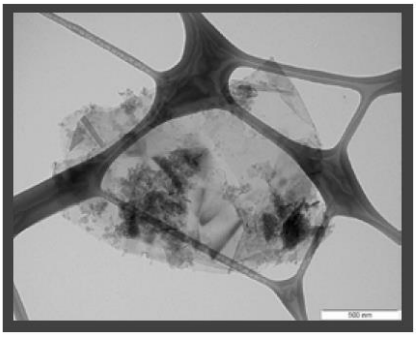

Figure 4.1 : Bond structure of graphene [46].

The characteristic that separates graphene from other carbon structures is that it comes from one dimensional atomic arrangement. Atoms are connected to each other only on the horizontal plane. The thickness of the structure in the vertical plane is only one atomic dimension. Thanks to this feature, the graphene is the first known single-layer structure [48].

In the future it is expected that widespread application of graphene based applications [49]. Research areas such as graphene-based transistor, battery, sensor production are available [50]. In addition, the structure where it joins the graphene also provides electrical and thermal conductivity [51; 52].

Due to the single-layer atomic structure of the graphene, it is difficult to mix homogeneously with other materials [47]. Therefore, it is chosen for blending experiments in the thesis. With this feature, it is aimed to observe the performance difference between mixing methods more clearly. The graphene used in the thesis is in "nanoplatelet (GnP)" structure. Technical information from the manufacturer is given in Table 4.1.

Table 4.1 : Technical information of the graphene material used in the thesis [46].

Brand	xGnP®
Structure	Nanoplatelet (GnP)
Surface area	500 m2/g
Density	0.2-0.4 g/cc
Attractive force	2-2.25 g/cc

Water based paint has been chosen as the material to be mixed with the graphene. It was used in the water-based finishing coat mixing experiments supplied as sample from DYO company. For each mixing method 125 microgram graphene and 100 ml pure water were pre-mixed via ultrasonic homogenizer (sonicator). The main reason for this pre-mixing is that the graphene particles which are very small are scattered around during the actual mixing application. Graphene particles in a very thin structure may be dangerous for health because they can penetrate the human body through the respiratory tract. With this pre-solving process, this risk has been removed. The graphene additive solution prepared with homogenizer was added into 500 ml water-based dye. Mixing was carried out for 30 minutes. The same experimental steps were applied for each mixing method explained in the beginning of this chapter. Attention has been paid to the fact that all mixing experiments are carried out under identical conditions. The resultant mixture was used for homogeneity analysis and material characterization analysis which will be described in the following chapters. Sample images of the mixing process are shown in Figure 4.2.

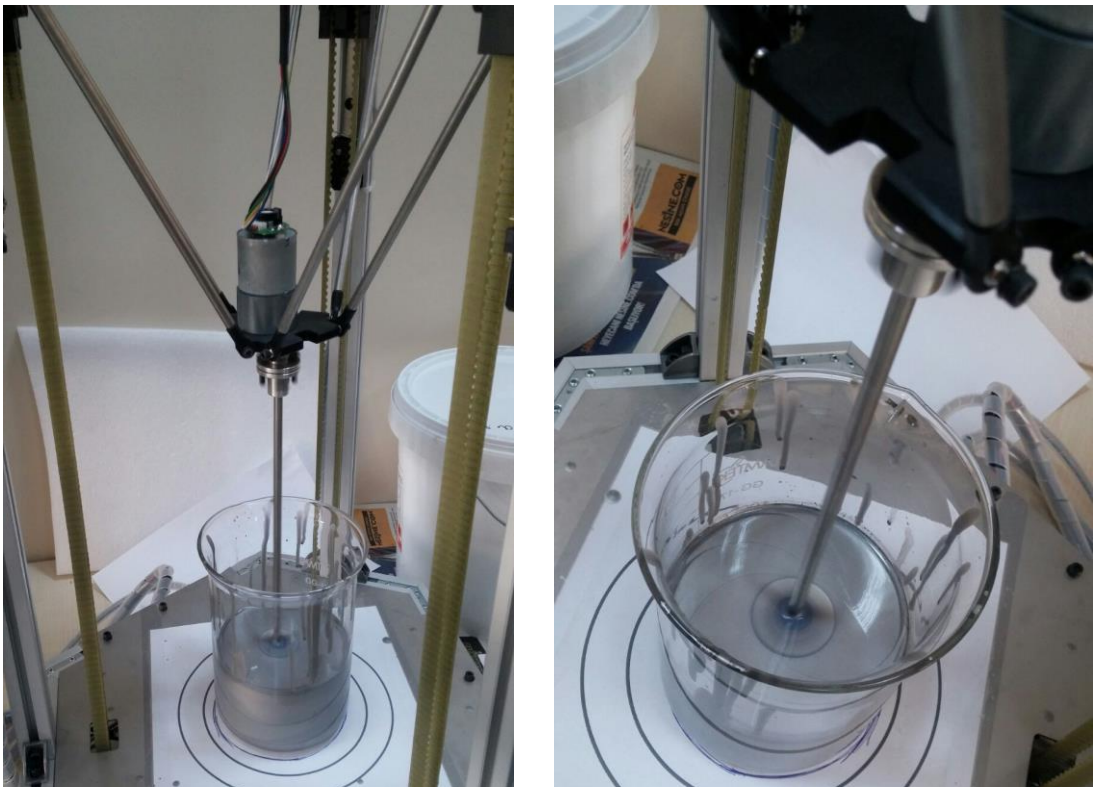

Figure 4.2 : Mixing graphene nanoplatelet with water-based dye.

4.2 Characterization

Characterization analyses of the obtained mixtures were handled by the “Fourier Transform Infrared Spectroscopy Analysis (FTIR)”, “Water contact angle measurements (WCA)” and “X-ray diffraction (XRD) Analysis”.

The FTIR-ATR analyses of samples are determined by using Thermo Scientific Nicolet 6700. Each sample were taken 64 scans and evaluated in the range of 500-4000 cm-1.

X-ray diffraction data were obtained with Philips X-Pert Pro, X-ray diffractometer. The diffractometer with Ni filtered CuKα radiation (l ¼ 1.54 Å) was operated in a step time 0, 05 in the range of 5-90 (2θ).

Contact angle measurements were performed by using a ThetaLite101, Biolin Scientific. A water droplet of 3 µL was added onto each sample surface using a testing syringe at ambient temperature.

4.2.1 Fourier transform infrared spectroscopy analysis

Infrared rays’ absorption or reflection spectrometry of the material were tested by Fourier Transform Infrared Spectroscopy Analysis (FTIR) [53]. The FTIR basically works as follows; a thin film is obtained from the sample to be tested. A full-spectrum light beam is sent from the infrared light source onto the sample. The beam of light passing through the other side of the sample is detected by a detector. The spectrum of this beam of light is plotted.

The light beam transmitted in the FTIR method strikes all the different molecules in the tested sample. Some rays hit to the molecules and pass through the opposite end of the reflection, while others are damped by molecules. The wavelength spectrum of the beam that each molecule damps or reflects is unique. With this feature, it is possible to differentiate each molecule within the test sample by FTIR analysis [54]. For example, the FTIR spectra of the graphene material in the graphene nanoplatelet (GnP) structure used in the thesis was found in the literature review and is shown in Figure 4.3.

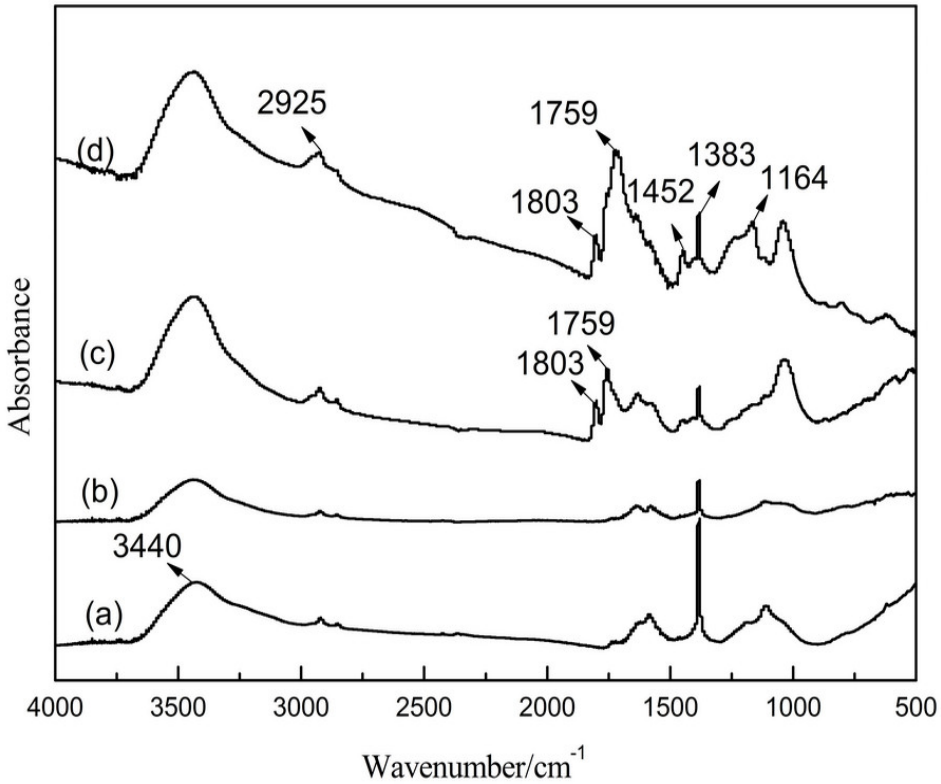

Figure 4.3 FTIR spectrum of graphen with different structures (a) MWCNTs-OH. (b) GnPs-OH. (c) MWCNTs-PACl. (d) MWCNTs/GnPs hybrit [55].

The FTIR spectrum graph of the GnP structure used in the thesis is shown as a line (b) in Figure 4.3, which is quoted from [55]. According to this spectrum, the graphene used in the thesis shows high absorbency at 1350-1500 wavelength/cm-1. This feature is used at the end of the chapter to evaluate the mixing results. Four different mixing scenarios and FTIR analyses for pure dye were carried out in İzmir Katip Çelebi University at Material Engineering Department laboratories. The obtained results are presented in Figure 4.4.

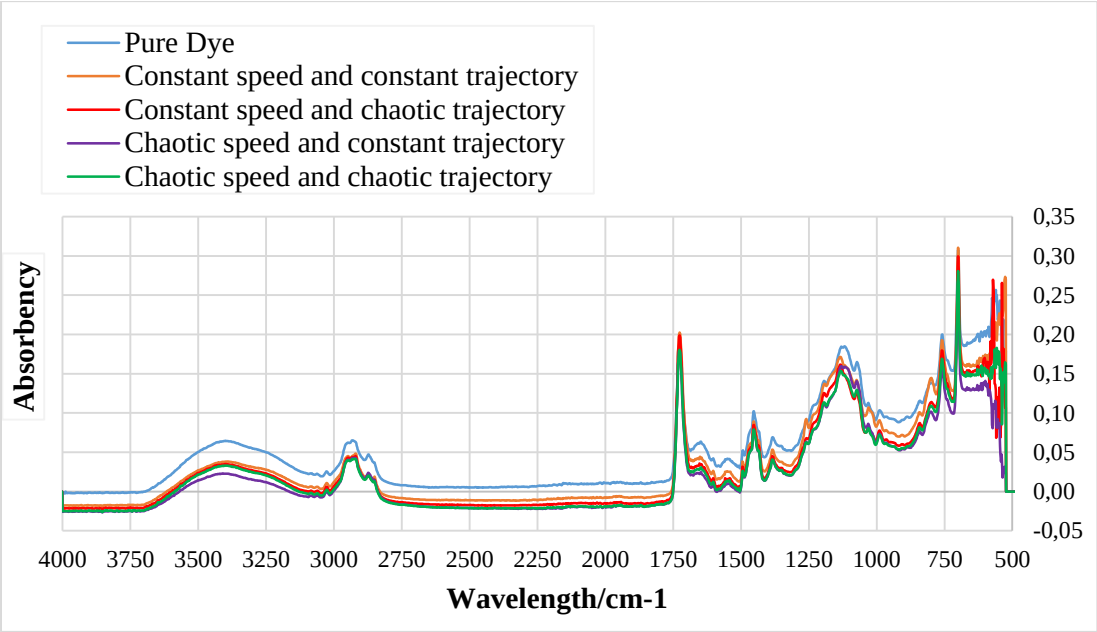

Figure 4.4 : FTIR analysis results of test samples (Full spectrum).

The graph in Figure 4.4 includes the full infrared light spectrum. For a more detailed and efficient analysis of the results it is necessary to take a closer look at the 1350-1500 wavelength/cm^{-1} range, where the absorption of the graphene is higher. This graph is shown in Figure 4.5 below.

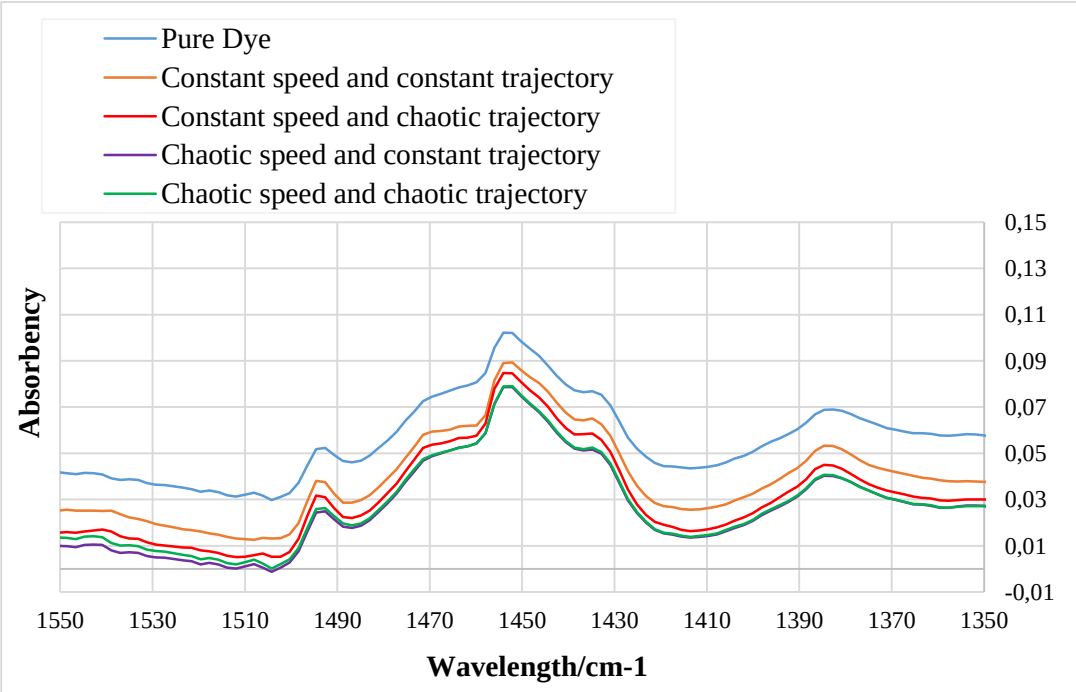

Figure 4.5 : FTIR analysis results of test samples (between 1350-1500 wavelength/cm-1).

As the homogeneity of the mixture increases, it is expected that the FTIR spectra will be differentiated more than the pure paint (blue line in Figure 4.5). According to the graphical results, the most different result from the pure dye was realized in the "chaotic speed and chaotic trajectory" scenario (green line in Figure 4.5) in the range of 1350-1500 wavelength/cm^{-1}. The mixing of "chaotic speed and constant trajectory" is very close to this result (purple line in Figure 4.5). “Constant speed, chaotic trajectory and “constant speed, constant trajectory” gave the lowest homogenous results. According to these data, the most homogenous mixing is achieved by the "chaotic speed and chaotic trajectory" and "chaotic speed and constant trajectory" methods. This homogeneity analysis is not sufficient to fully assess the success of the system, but it is an indication that the chaotic mixing method positively contributes to performance.

4.2.2 Water contact angle measurements

Contact angle analysis is a method of analysis that measures the wettability of the material. It is used to measure the mechanical characterization of materials. In the contact angle analysis, the sample taken from the material is transferred to a smooth flat surface in the form of a drop. As can be seen in Figure 4.6, the angle of this drop with the surface is measured.

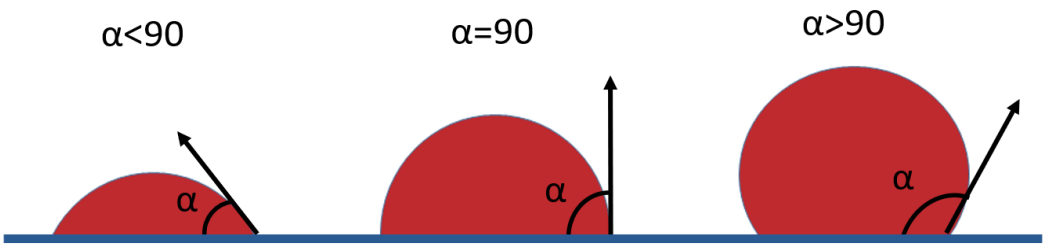

Figure 4.6 : Illustration of contact angle measurement.

As the wettability of the material changes, the shape and contact angle on the surface also changes significantly. In this characterization method, the contact angle of the pure dye, which is primarily used in the blending, is measured to obtain a reference value. The measurement is presented in Figure 4.7

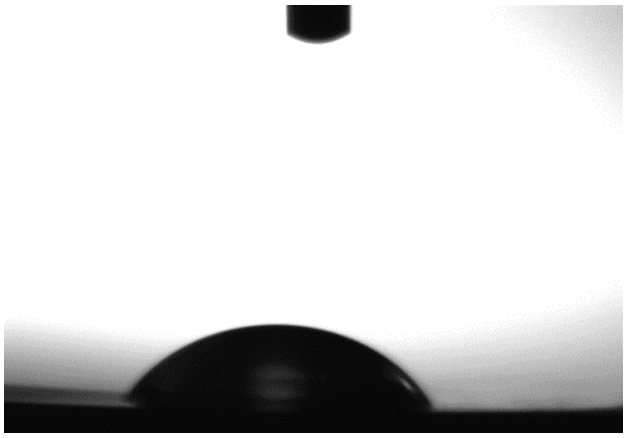

Figure 4.7 : Contact angle measurement of pure dye.

According to the measurement, the contact angle of pure dye was 65.00 °. The same test was carried out on the samples obtained by the four different mixing methods under the same conditions. The expected result from the test is that the contact angle value of the more homogeneous mixture is closer to contact angle value of pure dye. Figure 4.8 shows images of the contact angle analysis applied to all blending samples and Table 4.2 presents the measurement results.

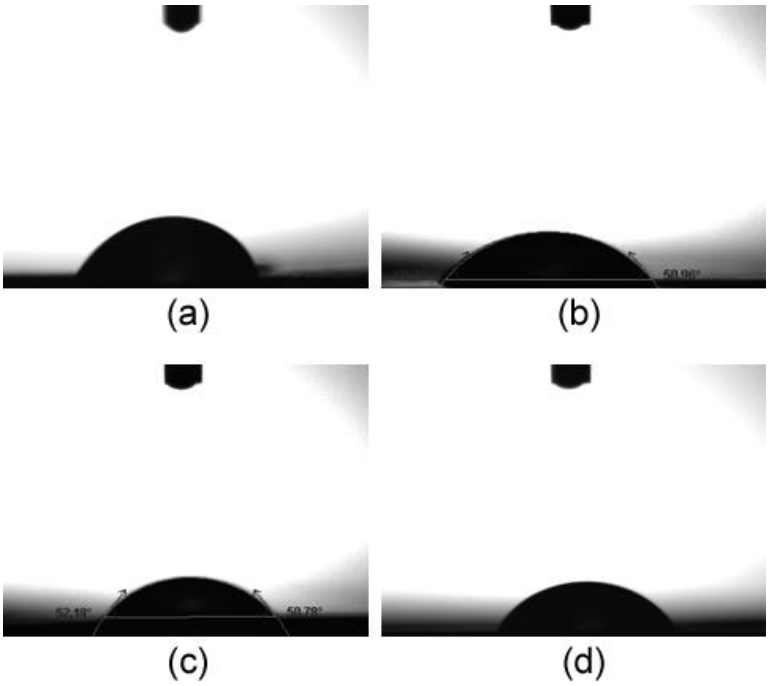

Figure 4.8 : Contact angle measurement of all blending methods (a) Constant speed and constant trajectory; (b) Constant speed and chaotic trajectory; (c) Chaotic speed and constant trajectory; (d) Chaotic speed and chaotic trajectory.

Table 4.2 : Contact angle values of all blending methods.

Sample	**Contact angle**
Pure dye	65.00°
Constant speed and constant trajectory	44.00°
Constant speed and chaotic trajectory	50.00°
Chaotic speed and constant trajectory	51.17°
Chaotic speed and chaotic trajectory	58.19°

More chaotical mixing increases the contact angle of the pure dye an it makes it less hydrophobic due to hydrophobic character of the graphene [56]. As the graphene is just mixed with chaotic mixing only in the mixer, it has better dispersion as the contact angle decreased to 50^0 values showing that better mixing was achieved. As the graphene particles in the mixture are homogeneously spread, the contact angle value of the mixture approaches the contact angle value of pure dye. If the particles in the mixture are not homogeneously dispersed and gathered at certain points, the droplets obtained from the sample will form different types of shapes on the smooth surface as shown in Figure 4.8. These results can be easily observed from both the visual and numerically. All results show that, "chaotic speed and chaotic trajectory" blending has the closest contact angle value to pure dye. There is no doubt that this mixing method is the most successful method according to these results.

4.2.3 X-ray diffraction (XRD) analysis

X-ray diffraction (or X-ray crystallography) is a method for determining the atomic and molecular structure of materials [57]. It is frequently used in chemistry, biology and material engineering fields. As, graphene is also a layered structure, XRD was used to identify the dispersion of the graphene layers in the water-based coatings [58]. In this method, the material is positioned in a tube and X-ray is transmitted. The atoms and molecules in the material deflect the transmitted X-rays with specific angles. The measurement of these deflection angles and the amount of density at these angles determine the atomic structures, bonds and other information in the material [59]. For example, the XRD graph of the graphene nanoplatelet structure obtained from the manufacturer is shown in Figure 4.9.

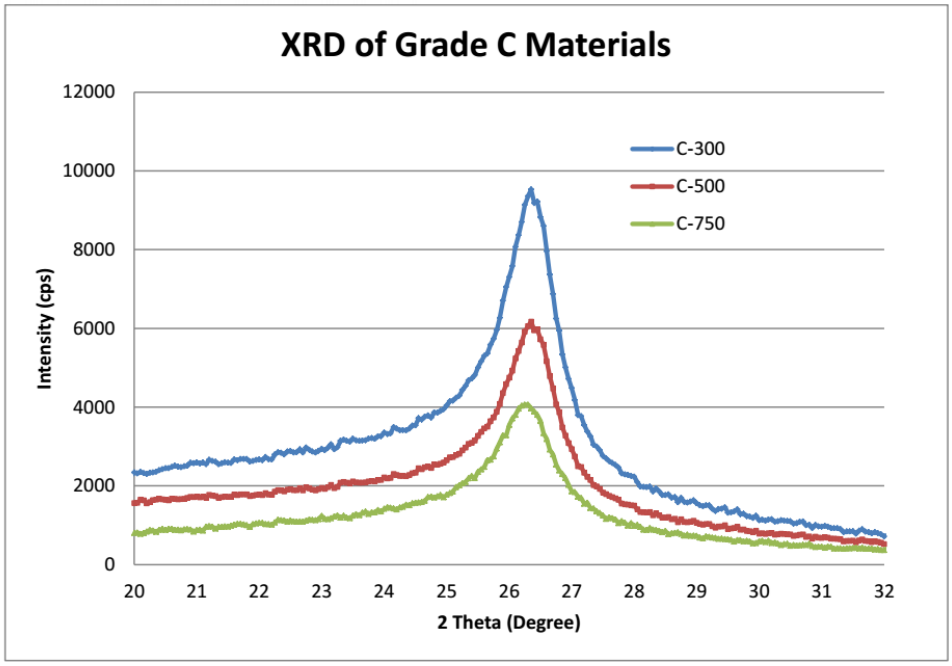

Figure 4.9 : X-ray crystallography graph of the graphene nanoplatelet [60].

As can easily be seen in Figure 4.9, the graphene shows a distinct peak at 26-27 degrees in XRD analysis.

To measure X-ray crystallography of all blending methods, the samples were prepared in specific forms. Samples were taken from the obtained mixtures and dried in thin film form. An example of this process can be seen from Figure 4.10.

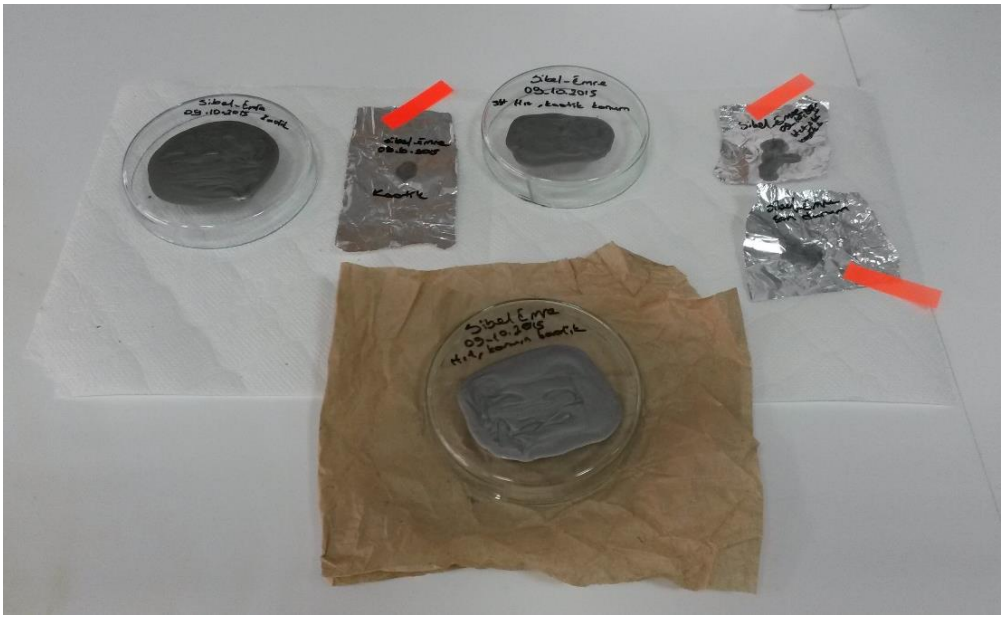

Figure 4.10 : Obtained thin film samples from mixtures.

After the films are obtained, XRD analysis was applied to the samples taken from pure dye and four different mixing scenarios as in previous analyses. The results are shown in Figures 4.11, 4.12, 4.13, 4.14 and 4.15.

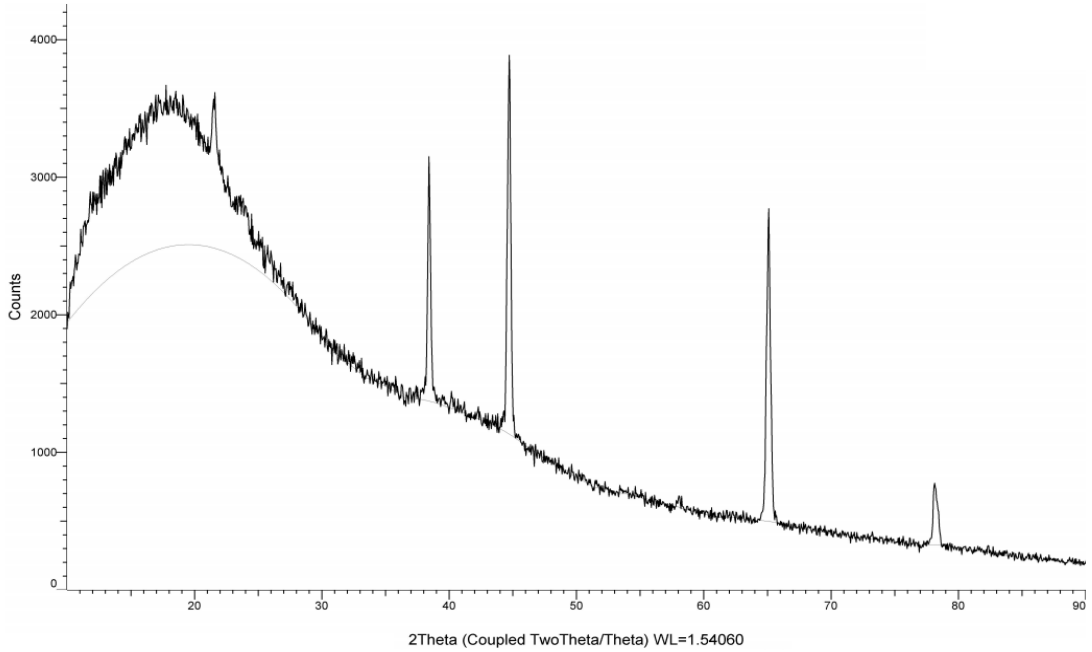

Figure 4.11 : XRD analysis of pure dye.

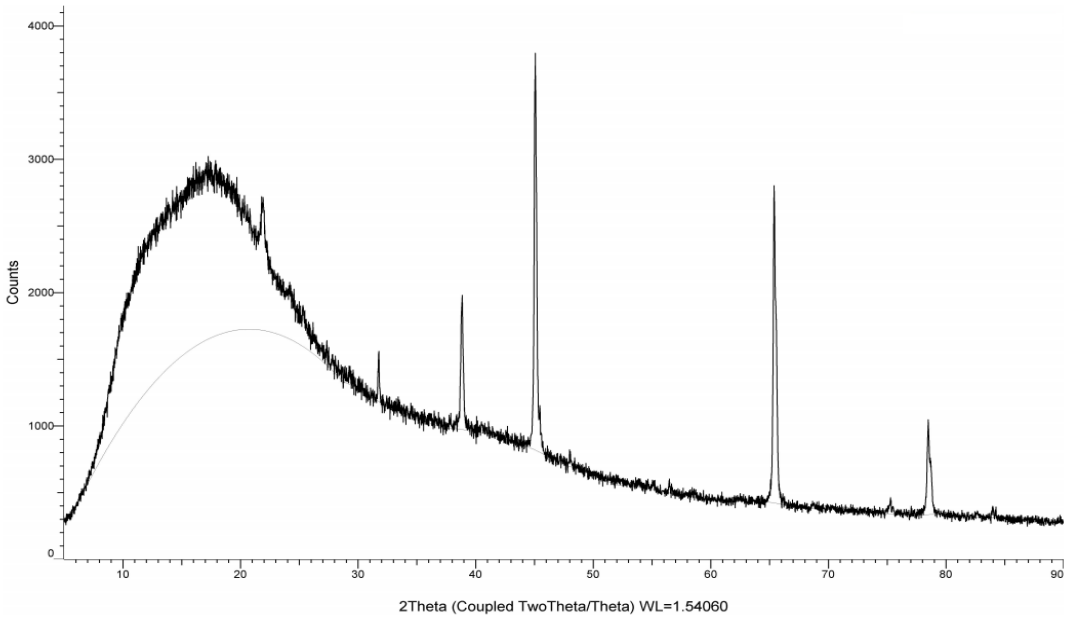

Figure 4.12 : XRD analysis of constant speed and constant trajectory.

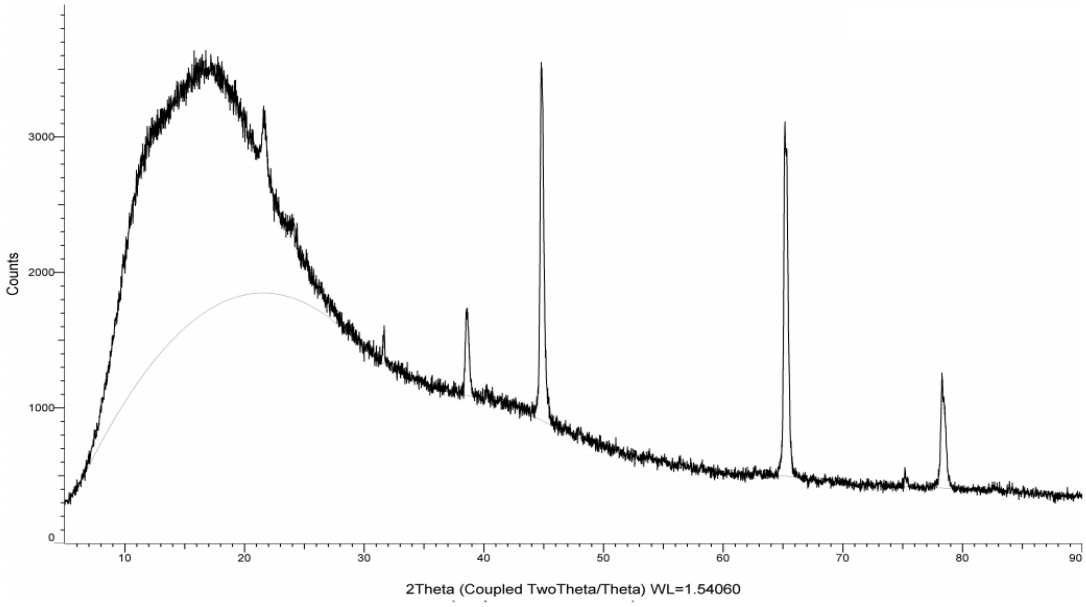

Figure 4.13 : XRD analysis of constant speed and chaotic trajectory.

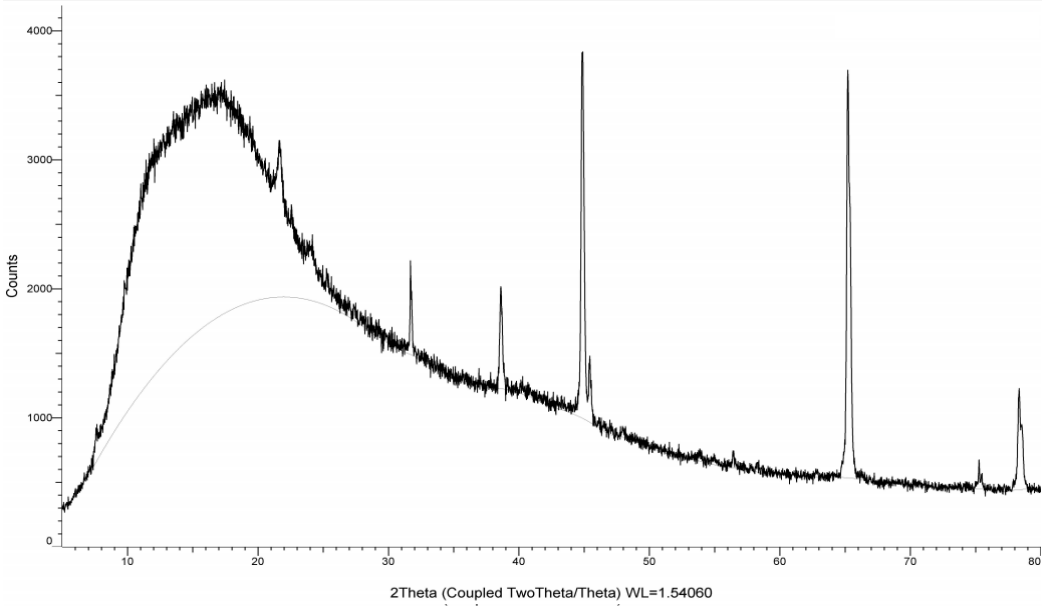

Figure 4.14 : XRD analysis of chaotic speed and constant trajectory.

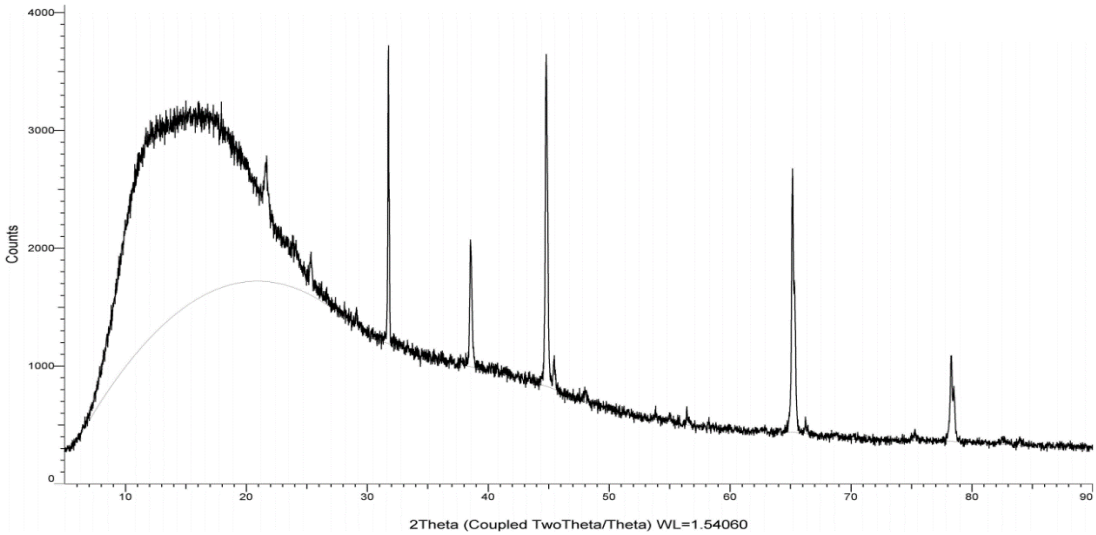

Figure 4.15 : XRD analysis of chaotic speed and chaotic trajectory.

There is not a peak at 30-35 degrees in the XRD analysis of the pure dye shown in Figure 4.11. However, a peak at 30-35 degrees is present in Figures 4.12, 4.13, 4.14 and 4.15. This peak belongs to the graphene material. As can be seen in Figure 4.11, the pure graphene exhibits a distinct peak at 26-27 degrees, but this peak after mixing with pure paint has shifted about 5 degrees. These peaks, which appear on the graphs, show the magnitude of how effectively the graphene penetrated in the dye. A peak of a higher value indicates that the substance is more successfully and effectively blended. The peak values at 30-35 degrees in the XRD results for the four different mixing scenarios are compiled in Table 4.3.

Table 4.3 : XRD analysis results.

Sample	**Peak value at 30-35 degree**
Constant speed and constant trajectory	1590
Constant speed and chaotic trajectory	1600
Chaotic speed and constant trajectory	2120
Chaotic speed and chaotic trajectory	3715

As presented in Figures 4.12, 4.13, 4.14, 4.15 and Table 4.3, it has been determined that the “chaotic speed and chaotic trajectory” method is the most effective mixing method of graphene in pure dye. More detailed comments are included in the results chapter.

4.3 Energy Consumption Analyses

In the mixing experiments of the graphene, the electricity consumptions of the whole blending system were measured. Measurements were made separately for four different mixing scenarios.

The energy measurement data was obtained by measuring the amount of electric energy consumed by the delta robot mixer system. The measurement was taken from 220V power connection at the input of the system. Thus, the total energy consumption of the delta robotic blender system was measured. The power consumption of four scenarios and stand-by mode are presented in Figure 4.16.

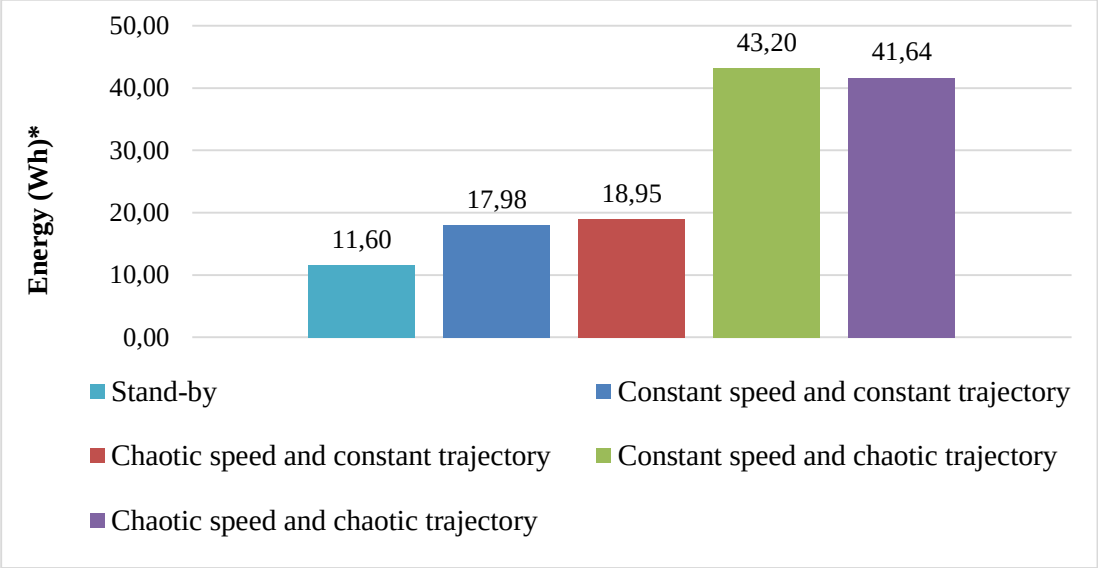

Figure 4.16 : Energy consumption analyses of all blending methods. (* Energy (Wh) is calculated by multiplying between average power and time.)

As can be seen from Figure 4.16, the methods where the trajectory is changed, the consumption of electric energy is determined to be increased. The main reason for this increase is the stepper motors on the delta robot-based blender. Stepping motors do not work when position is constant. In the chaotic mode, the stepper motors operate continuously. This difference has also been identified as the main source of the increase in energy consumption. However, the energy measurement is not enough to evaluate the system alone. The work done for the energy consumed while the system is being tested is also to be considered. Comments on this situation are provided in the conclusion chapter of the thesis.

5. CONCLUSION

A novel system has been designed and it is expected to bring innovations in the chemical-material sectors with this thesis. Firstly, chaotic systems in the literature have been examined and the most suitable ones for the thesis have been integrated into the system. These chaotic systems are re-elaborated for the delta robot-based mixer and are adapted to the system by calculating the relevant parameters. Two different and independent chaotic systems have been used because the delta robot can move both in three-dimensional coordinate plane and can blend with the DC motor with different operating scenarios. To evaluate the performance of the system, the graphene material was mixed with water-based dye for each scenario and the obtained samples were evaluated by different measurement methods.

Nanotechnology is a field where much research is done nowadays. Nanostructures are usually mixed with different polymers, resins and liquid systems in the form of nanocomposite. While nanocomposite and nanotechnology promise many field of research, it is very difficult to obtain a stable nanocomposite form. A new system has been designed which enables both time-saving and efficient nanocomposite form preparation.

Nanocomposites are more effectively mixed by our system according to Fourier Transform Infrared Spectroscopy (FTIR), Contact Angle, X-ray Diffraction (XRD) analyses. In the FTIR results, the result obtained most differently from pure dye in the range of 1350-1500 wavelength/cm^{-1} was realized in the “chaotic speed and chaotic trajectory” scenario. The contact angle measurements show that the most homogeneous mixture was also obtained again in the “chaotic speed and chaotic trajectory” scenario. In addition to these results, the highest density of the graphene material in the XRD results was obtained by the “chaotic speed and chaotic trajectory” method. All of the experiments and analyses definitely shows us “chaotic speed and chaotic trajectory” method is the most successful method. Chaotic change of position

and speed ensures the most homogeneous mixture as expected the design stage of the system.

For energy measurements, an increase in energy consumption was observed when the position of the propeller changed. The main reason for this increase is that the stepper motors in the system. They actively work in the mixing methods where the position changes. These motors, as well as their engine drivers, have led to increased consumption of electrical energy in the system. It is presumed that this deficiency can be overcome by different chaotic mixer designs. This problem can be overcome by designing the mechanism for changing position in the system by using other motion systems such as pneumatic systems, piston systems, etc. instead of step motors.

Effective mixing of fluids in industrial work is known as an important design task. The difficulty of this task makes it a popular research and development topic. Due to these reasons, it is considered that the system which is designed for this study will find important usage areas in the industry. In the future, it is planned to add additional components such as the use of more than one mixer motor in the system or the tilting of the mixer motor. In addition, remote control over TCP/IP or RFID and integration with PLC systems are considered for better integration of the system in industrial usage.

This thesis was supported in part by the Scientific and Technological Research Council of Turkey (TÜBİTAK) under Grant 114E432.

REFERENCES

[1] Paul, E. L., Atiemo-Obeng, V. A., & Kresta, S. M. (2004). *Handbook of industrial mixing: science and practice*. John Wiley & Sons.

[2] Şahin, S., & Güzeliş, C. (2013). A Dynamical State Feedback Chaotification Method With Application on Liquid Mixing. *Journal of Circuits, Systems and Computers*, *22*(07), 1350059. https://doi.org/10.1142/S021812661350059X

[3] Rey, L., & Clavel, R. (1999). The Delta Parallel Robot (pp. 401–417). Springer, London. https://doi.org/10.1007/978-1-4471-0885-6_29

[4] Company, O., & Pierrot, F. (2002). Modelling and design issues of a 3-axis parallel machine-tool. *Mechanism and Machine Theory*, *37*(11), 1325–1345. https://doi.org/10.1016/S0094-114X(02)00040-X

[5] Asgari, M., Ardestani, M. A., & Asgari, M. (2013). Dynamics and control of a novel 3-DoF spatial parallel robot. In *2013 First RSI/ISM International Conference on Robotics and Mechatronics (ICRoM)* (pp. 183–188). IEEE. https://doi.org/10.1109/ICRoM.2013.6510102

[6] Březina, L., Holub, M., Cintula, L., & Kovar, J. (2013). Delta Robot Design. *Solid State Phenomena*, *198*, 9–14. https://doi.org/10.4028/www.scientific.net/SSP.198.9

[7] Connolly, C. (2007). ABB high-speed picking robots establish themselves in food packaging. *Industrial Robot: An International Journal*, *34*(4), 281–284. https://doi.org/10.1108/01439910710749591

[8] Deblaise, D., & Maurine, P. (2005). Effective geometrical calibration of a delta parallel robot used in neurosurgery. In *2005 IEEE/RSJ International Conference on Intelligent Robots and Systems* (pp. 1313–1318). IEEE. https://doi.org/10.1109/IROS.2005.1545081

[9] Allen, B. F., Jordan, B., Pannell, W., Lewis, C., Dutson, E., & Faloutsos, P. (2010). Laparoscopic Surgical Robot for Remote In Vivo Training. *Advanced Robotics*, *24*(12), 1679–1694. https://doi.org/10.1163/016918610X522513

[10] Ishitobi, M., & Liang, S. (2001). Zeros of a multivariable discrete-time system with fractional-order hold. *System Structure and Control 2001, Vols 1 and 2*, 591–596.

[11] Brooks, B. J., Arif, K. M., Dirven, S., & Potgieter, J. (2017). Robot-assisted 3D printing of biopolymer thin shells. *The International Journal of Advanced Manufacturing Technology*, *89*(1–4), 957–968.

https://doi.org/10.1007/s00170-016-9134-y

[12] Hirano, J., Tanaka, D., Watanabe, T., & Nakamura, T. (2014). Development of delta robot driven by pneumatic artificial muscles. In *2014 IEEE/ASME International Conference on Advanced Intelligent Mechatronics* (pp. 1400–1405). IEEE. https://doi.org/10.1109/AIM.2014.6878278

[13] Demiroğlu, A.E. Kavur, C. Güzeliş, Ö. Başer, M.Ö. Seydibeyoğlu, S. S. (2016). A Novel Approach to Prepare Graphene Nanocomposites via Chaotic Mixing. In *14th International Symposium on Bioplastics, Biocomposites and Biorefining (ISBBB 2016)*. Guelph, Canada. Retrieved from https://www.researchgate.net/publication/308054660_A_Novel_Approach_to_Prepare_Graphene_Nanocomposites_via_Chaotic_Mixing?channel=doi&linkId=57d840e908ae601b39afa0b8&showFulltext=true

[14] Kavur, A. E., Demiroglu, S., Seydibeyoglu, M. O., Baser, O., Guzelis, C., & Sahin, S. (2016). Design and implementation of chaotic system based robust delta robot for blending graphene nanoplatelets. In *2016 21st International Conference on Methods and Models in Automation and Robotics, MMAR 2016*. https://doi.org/10.1109/MMAR.2016.7575139

[15] Papazoglou, E. S., & Parthasarathy, A. (2007). BioNanotechnology. *Synthesis Lectures on Biomedical Engineering*, *2*(1), 1–139. https://doi.org/10.2200/S00051ED1V01Y200610BME007

[16] Sahoo, S. K., & Labhasetwar, V. (2003). Nanotech approaches to drug delivery and imaging. *Drug Discovery Today*, *8*(24), 1112–1120. Retrieved from http://www.ncbi.nlm.nih.gov/pubmed/14678737

[17] Rahman, M., Akhter, S., Ahmad, M. Z., Ahmad, J., Addo, R. T., Ahmad, F. J., & Pichon, C. (2015). Emerging advances in cancer nanotheranostics with graphene nanocomposites: opportunities and challenges. *Nanomedicine*, *10*(15), 2405–2422. https://doi.org/10.2217/nnm.15.68

[18] Mogharabi, M., Abdollahi, M., & Faramarzi, M. (2014). Safety concerns to application of graphene compounds in pharmacy and medicine. *DARU Journal of Pharmaceutical Sciences*, *22*(1), 23. https://doi.org/10.1186/2008-2231-22-23

[19] Hsu, Y.-H., Hsieh, H.-L., Viswanathan, G., Voon, S. H., Kue, C. S., Saw, W. S., … Chung, L. Y. (2017). Multifunctional carbon-coated magnetic sensing graphene oxide-cyclodextrin nanohybrid for potential cancer theranosis. *Journal of Nanoparticle Research*, *19*(11), 359. https://doi.org/10.1007/s11051-017-4054-9

[20] Chhabra, R. P., & Richardson, J. F. (John F. (1999). *Non-Newtonian flow in the process industries : fundamentals and engineering applications*. Butterworth-Heinemann.

[21] Tropea, C., Yarin, A. L., & Foss, J. F. (2007). *Springer handbook of experimental fluid mechanics*. Springer Science+Business Media.

[22] Chhabra, R. P. (2007). *Bubbles, drops, and particles in non-Newtonian fluids*. Hoboken : CRC Taylor & Francis. Retrieved from http://www.worldcat.org/title/bubbles-drops-and-particles-in-non-

newtonian-fluids/oclc/437171474

[23] Grainger, S., & Jane Blunt. (1998). Engineering Coatings: Design and Application, 319. Retrieved from https://www.sciencedirect.com/science/book/9781855733695

[24] Lawrence, C. J., & Zhou, W. (1991). Spin coating of non-Newtonian fluids. *Journal of Non-Newtonian Fluid Mechanics*, *39*(2), 137–187. https://doi.org/10.1016/0377-0257(91)80010-H

[25] Britten, J. A., & Thomas, I. M. (1992). Non-Newtonian flow effects during spin coating large-area optical coatings with colloidal suspensions. *Journal of Applied Physics*, *71*(2), 972–979. https://doi.org/10.1063/1.351323

[26] Kim, K. J., & Kwak, H. S. (2012). Analytic Study of Non-Newtonian Double Layer Coating Liquid Flows in Optical Fiber Manufacturing. *Applied Mechanics and Materials*, *224*, 260–263. https://doi.org/10.4028/www.scientific.net/AMM.224.260

[27] Pruna, A., Pullini, D., & Soanca, A. (2017). Graphene-Based Coatings for Dental Implant Surface Modification. In *Carbon-related Materials in Recognition of Nobel Lectures by Prof. Akira Suzuki in ICCE* (pp. 103–116). Cham: Springer International Publishing. https://doi.org/10.1007/978-3-319-61651-3_6

[28] Pattnaik, S., Swain, K., & Lin, Z. (2016). Graphene and graphene-based nanocomposites: biomedical applications and biosafety. *Journal of Materials Chemistry B*, *4*(48), 7813–7831. https://doi.org/10.1039/C6TB02086K

[29] Jenekhe, S. A., & Schuldt, S. B. (1984). Coating flow of non-Newtonian fluids on a flat rotating disk. *Industrial & Engineering Chemistry Fundamentals*, *23*(4), 432–436. https://doi.org/10.1021/i100016a009

[30] Seydibeyoglu, M. O., Isci, S., Gungor, N., Ece, O. I., & Guner, F. S. (2010). Preparation of Polyurethane/Hectorite, Polyurethane/Montmorillonite, and Polyurethane/Laponite Nanocomposites without Organic Modifiers. *Journal of Applied Polymer Science*, *116*(2), 832–837. https://doi.org/10.1002/app.31532

[31] Chau, K. T., & Ye, S. (2007). Chaoization of DC motors for industrial mixing. *IEEE Transactions on Industrial Electronics*, *54*(4), 2024. https://doi.org/10.1109/TIE.2007.895150

[32] Zhang, Z., & Chen, G. (2008). Liquid mixing enhancement by chaotic perturbations in stirred tanks. *Chaos, Solitons & Fractals*, *36*(1), 144–149. https://doi.org/http://dx.doi.org/10.1016/j.chaos.2006.06.024

[33] Şahin, S., & Güzeliş, C. (2012). Engineering applications of a dynamical state feedback chaotification method. *AIP Conference Proceedings*, *1479*(1), 686–690. https://doi.org/doi:http://dx.doi.org/10.1063/1.4756227

[34] De Gennes, P. G. (1985). Wetting: Statics and dynamics. *Reviews of Modern Physics*, *57*(3), 827–863. https://doi.org/10.1103/RevModPhys.57.827

[35] Yuan, Y., & Lee, T. R. (2013). Contact Angle and Wetting Properties. In G.

Bracco & B. Holst (Eds.) (pp. 3–34). Berlin, Heidelberg: Springer Berlin Heidelberg. https://doi.org/10.1007/978-3-642-34243-1_1

[36] Strogatz, S. H. (1994). Nonlinear dynamics and chaos with applications to physics, chemistry and engineering. *American Journal of Respiratory and Critical Care Medicine*, *168*(4), 425–430. Retrieved from https://books.google.com.tr/books/about/Nonlinear_Dynamics_And_Chaos.html?id=PHmED2xxrE8C&redir_esc=y

[37] Lorenz, E. N. (1963, March). Deterministic Nonperiodic Flow. *Journal of the Atmospheric Sciences*. https://doi.org/10.1175/1520-0469(1963)020<0130:DNF>2.0.CO;2

[38] Chua, L. O., Wu, C. W., Huang, A., & Guo-Qun, Z. (1993). A universal circuit for studying and generating chaos. I. Routes to chaos. *IEEE Transactions on Circuits and Systems I: Fundamental Theory and Applications*, *40*(10), 732–744. https://doi.org/10.1109/81.246149

[39] Leipnik, R. B., & Newton, T. A. (1981). Double strange attractors in rigid body motion with linear feedback control. *Physics Letters A*, *86*(2), 63–67. https://doi.org/10.1016/0375-9601(81)90165-1

[40] Sheu, L. J., Chen, H. K., Chen, J. H., Tam, L. M., Chen, W. C., Lin, K. T., & Kang, Y. (2008). Chaos in the Newton-Leipnik system with fractional order. *Chaos Solitons & Fractals*, *36*(1), 98–103. https://doi.org/10.1016/j.chaos.2006.06.013

[41] Chen Tetsushi, G. U. (1999). Yet Another Chaotic Attractor. *International Journal of Bifurcation and Chaos*, *09*(07), 1465–1466. https://doi.org/doi:10.1142/S0218127499001024

[42] Rössler, O. E. (1976). An equation for continuous chaos. *Physics Letters A*, *57*(5), 397–398. https://doi.org/10.1016/0375-9601(76)90101-8

[43] Friman, O., Hindennach, M., & Peitgen, H.-O. (2008). Template-based multiple hypotheses tracking of small vessels. In *2008 5th IEEE International Symposium on Biomedical Imaging: From Nano to Macro* (pp. 1047–1050). IEEE. https://doi.org/10.1109/ISBI.2008.4541179

[44] Şahin, S., & Güzeliş, C. (2016). Online Learning ARMA Controllers With Guaranteed Closed-Loop Stability. *IEEE Transactions on Neural Networks and Learning Systems*, *27*(11), 2314–2326. https://doi.org/10.1109/TNNLS.2015.2480764

[45] Kocaoglu, A., & Guzelis, C. (2014). Model-based robust chaotification using sliding mode control. *Turkish Journal of Electrical Engineering and Computer Science*. Retrieved from http://dergipark.ulakbim.gov.tr/tbtkelektrik/article/view/5000106509

[46] Pharmingen, B. D. (2010). Technical Data Sheet. *XGnP Graphene Nanoplatelets*. https://doi.org/tttt

[47] Zhu, Y., Murali, S., Cai, W., Li, X., Suk, J. W., Potts, J. R., & Ruoff, R. S. (2010). Graphene and graphene oxide: synthesis, properties, and applications. *Advanced Materials (Deerfield Beach, Fla.)*, *22*(35), 3906–

3924. https://doi.org/10.1002/adma.201001068

[48] Castro Neto, A. H., Guinea, F., Peres, N. M. R., Novoselov, K. S., & Geim, A. K. (2009). The electronic properties of graphene. *Reviews of Modern Physics*, *81*(1), 109–162. https://doi.org/10.1103/RevModPhys.81.109

[49] Geim, A. K., & Novoselov, K. S. (2007). The rise of graphene. *Nature Mater.*, *6*(3), 183–191. https://doi.org/10.1038/nmat1849

[50] Lancellotti, L., Polichetti, T., Ricciardella, F., Tari, O., Gnanapragasam, S., Daliento, S., & Di Francia, G. (2012). Graphene applications in Schottky barrier solar cells. *Thin Solid Films*, *522*, 390–394. https://doi.org/10.1016/j.tsf.2012.09.040

[51] Mann, C. J., Yu, L., & Kim, M. K. (2006). Movies of cellular and sub-cellular motion by digital holographic microscopy. *Biomedical Engineering Online*, *5*, 21. https://doi.org/10.1186/1475-925X-5-21

[52] Shahil, K. M. F., & Balandin, A. A. (2012). Thermal properties of graphene and multilayer graphene: Applications in thermal interface materials. *Solid State Communications*, *152*(15), 1331–1340. https://doi.org/10.1016/j.ssc.2012.04.034

[53] Lin, S. Y., & Dence, C. W. (1989). Methods in Lignin Chemistry. In S. Y. Lin & C. W. Dence (Eds.), *Journal of Chemical Information and Modeling* (Vol. 53, pp. 83–109). Berlin, Heidelberg: Springer Berlin Heidelberg. https://doi.org/10.1017/CBO9781107415324.004

[54] Salzer, R. (2008). Peter R. Griffiths, James A. de Haseth: Fourier transform infrared spectrometry (2nd edn.). *Analytical and Bioanalytical Chemistry*, *391*(7), 1–2. https://doi.org/10.1007/s00216-008-2144-3

[55] Jia, Y., Yu, K., & Qian, K. (2013). Facile approach to prepare multi-walled carbon nanotubes/graphene nanoplatelets hybrid materials. *Nanoscale Research Letters*, *8*(1), 243. https://doi.org/10.1186/1556-276X-8-243

[56] Monetta, T., Acquesta, A., & Bellucci, F. (2015). Graphene/Epoxy Coating as Multifunctional Material for Aircraft Structures. *Aerospace*, *2*(3), 423–434. https://doi.org/10.3390/aerospace2030423

[57] Giacovazzo, C. (2002). *Fundamentals Of Crystallography* (Vol. 2). Oxford University Press.

[58] Chieng, B., Ibrahim, N., Yunus, W., Hussein, M., Then, Y., & Loo, Y. (2014). Effects of Graphene Nanoplatelets and Reduced Graphene Oxide on Poly(lactic acid) and Plasticized Poly(lactic acid): A Comparative Study. *Polymers*, *6*(8), 2232–2246. https://doi.org/10.3390/polym6082232

[59] Clegg, A. J., William, B., Cole, J. M., Evans, J. S. O., Main, P., Parsons, S., & Watkin, D. J. (2009). *Crystal Structure Analysis: Principles and Practice*. Oxford University Press.

[60] XnP Sciences. (2011). *Characterization of xGnP ® Grade C Materials*.

CURRICULUM VITAE

Ali Emre Kavur was born in August 1987, in Izmir, Turkey. He completed his undergraduate education in Izmir Institute of Technology at department of Electronic and Communication Engineering in 2011. He completed his first master degree in Dokuz Eylül University at department of Electrical and Electronic Engineering in 2014. During his education, he worked on projects related with image processing and control systems fields. His PhD education continues in Dokuz Eylül University about medical image processing field.

List of Research Projects:

1. TUBITAK EEEAG 116E133 (Jan 2017 – Apr 2019)

Development of Brushlet Transform Based Parametric Transfer Function Specification and Segmented Data Compression Methods and Their Integration to a DICOM Compatible Presentation State Object for Effective 3D Visualization.

Supervisor: Associate Prof. Dr. Alper SELVER

Dokuz Eylul University, Department of Electrical-Electronic Eng. İzmir, Turkey

2. TUBITAK EEEAG 114E432 (Sep 2014 - Sep 2016)

Design and implementation of chaotic system based robust delta robot liquid mixing.

Supervisor: Associate Prof. Dr. Savas SAHIN

Izmir Katip Celebi Universitesi, Electrical Electronics Eng., İzmir, Turkey

3. TUBITAK EEEAG 112E032 (Dec 2013 - Sep 2014)

Segmentation and three dimensional visualization of abdominal organs for advanced medical analysis from MR images using multi-level hierarchical classification

Supervisor: Associate Prof. Dr. Alper SELVER

Dokuz Eylul University, Department of Electrical-Electronic Eng. İzmir, Turkey

List of Publications:

1. **Ali Emre Kavur**, Sibel Demiroğlu, M. Özgür Seydibeyoğlu,Savas Sahin, (2016), Design and Implementation of Chaotic System Based Robust Delta Robot for Blending Graphene Nanoplatelets, Methods and Models in Automation and Robotics (MMAR), 2016 21st International Conference on (IEEE Conference Publications), DOI: 10.1109/MMAR.2016.7575139
2. Savas Sahin, Mutlu Bayraktar, **Ali Emre Kavur**, Kubra Evren Sahin, (2016), Gerçek Zamanlı EMG Verileri ile DC Motor Kontrolü, XX. Biyomedikal Mühendisliği Ulusal Toplantı (Uluslararası Katılımlı) BIYOMUT 2016, DOI: 10.19113/sdufbed.06905
3. Sibel Demiroğlu, **Ali Emre Kavur**, Cüneyt Güzeliş, Savas Sahin, (2016), A Novel Approach to Prepare Graphene Nanocomposites via Chaotic Mixing, Guelph, Canada, 14th International Symposium on Bioplastics, Biocomposites & Biorefining, DOI:10.13140/RG.2.2.32539.46888
4. Nail Akçura, **Ali Emre Kavur**, Savas Sahin, (2016), HMI based Servo Motor Application for Control Laboratory, Conference: International Conference on Research in Education and Science (ICRES), At Bodrum, Turkey
5. **Ali Emre Kavur**, Nail Akçura, Savas Sahin, (2016), Design and Implementation of CanBus based PLC and Inverter Control for AC Motor Application, Conference: International Conference on Research in Education and Science (ICRES), At Bodrum, Turkey
6. M. Alper Selver, **Ali Emre Kavur**, (2015), Implementation and use of 3D pairwise geodesic distance fields for seeding abdominal aortic vessels, International Journal of Computer Assisted Radiology and Surgery. DOI: 10.1007/s11548-015-1321-z
7. Esref Selvi, M. Alper Selver, **Ali Emre Kavur**, Cüneyt Güzeliş, Oğuz Dicle, (2015), Batin Bölgesi Organlarinin MR Görüntülerinden Çok Aşamali Hiyerarşik Siniflama İle Bölütlenmesi, Journal of the Faculty of Engineering and Architecture of Gazi University, DOI: 10.17341/gummfd.93803